ADAPTIVE IMPEDANCE RELAYS

by

Sunny L. K. Chan

A thesis
presented to the University of Manitoba
in partial fulfillment of the
requirement for the degree of

Master of Science

in Department of Electrical and Computer Engineering
University of Manitoba
Winnipeg, Manitoba

ISBN 0-315-78046-0

ADAPTIVE IMPEDANCE RELAYS

BY

SUNNY L.K. CHAN

A Thesis submitted to the Faculty of Graduate Studies of the University of Manitoba in partial fulfillment of the requirements for the degree of

MASTER OF SCIENCE

ABSTRACT

An adaptive method for improving the performance of digital distance protection during the conditions of ground–fault resistance carrying current from the remote source is presented. This adaptive method is shown to possess the ability to alter the remote reactance boundary to accommodate more closely the measured reactance under such conditions. Also, a new method for dealing with the problem caused by additional taps on the transmission system is described. It is shown that the accuracy of fault measurement can be maintained under such circumstances. The protection methods are tested by simulating the operation of the digital relay on an UNIX based SUN workstation. These simulations have verified that the adaptive protection method is feasible.

ACKNOWLEDGEMENTS

I wish to thank my advisor Professor Peter McLaren for his guidance. I also wish to thank Mr. Dave Fedirchuk for providing the necessary information for the simulation model. I would like to thank my parents for their patience and support. My thanks go also to my friends whose help made it possible to complete this thesis. Lastly, I am grateful to Manitoba Hydro where financial assistance facilitated the research.

TABLE OF CONTENT

LIST OF FIGURES

LIST OF TABLES

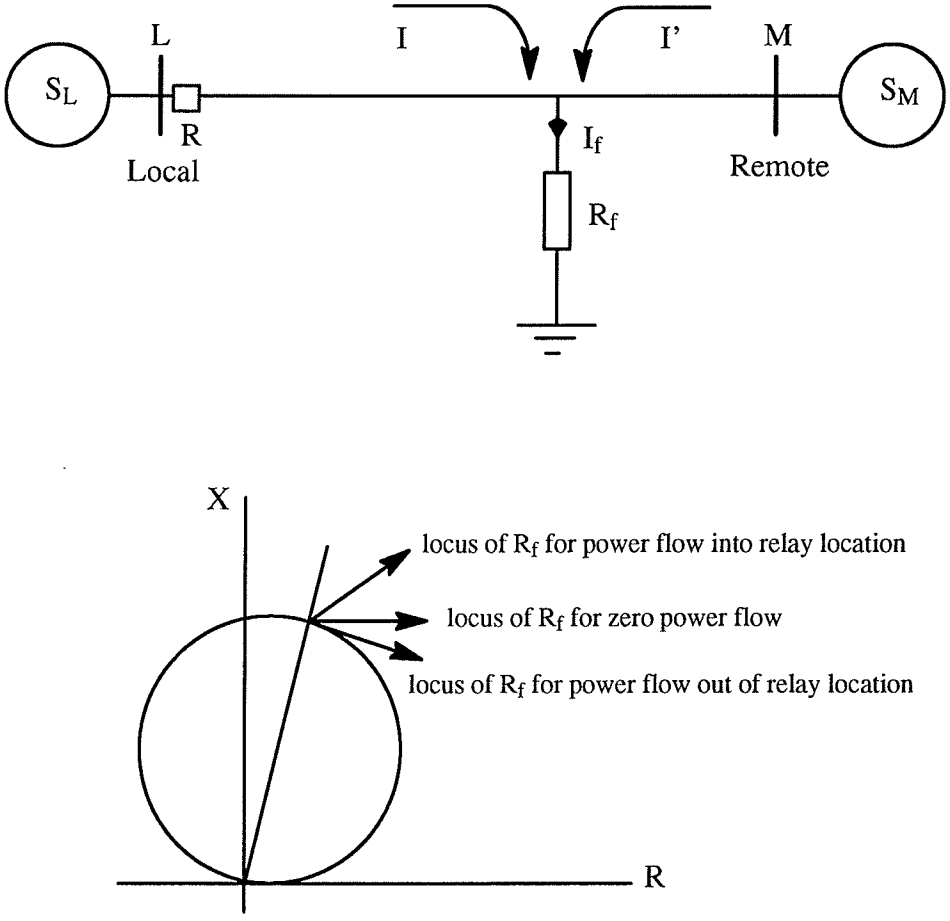

Figure 1.1 Impedance locus with different power flow direction

CHAPTER 1

INTRODUCTION

1.1 Objective

A desire for a more accurate and faster power system protection method and device is always present among relay engineers. In recent years, strong interest in the development of digital relaying systems has been indicated by the numerous amount of technical articles on this subject. With the growing trend toward the use of digital relaying systems, the need for the development of appropriate protection algorithms has increased. It is the goal of this thesis to provide a new protection algorithm which will meet some of these needs.

1.2 Problem

The impedance relay plays an important role in the modern transmission line protection system. In fact, it has been the major common element in a wide range of protection schemes. Nevertheless, for a fault impedance close to the remote boundary (80% of protected line) fault resistance (R_f) carrying current from the the remote source can cause an in–zone fault to look outside the trip boundary if the prefault power flow is into the relay location and an out of zone fault to look inside the boundary for prefault power flow out of the relay location. Figure 1.1 on page 1A shows a simple power transmission system with a typical "mho" boundary for a zone 1 protection and the impedance locus with different power flow direction for the system.

Furthermore, when there are taps connected on the transmission line at intermediate points, the power system becomes a multiple–earthed system if the high–voltage star windings of the transformers are grounded. The additional taps on the system alter the zero–sequence impedance of the original network. Under these circumstances an earth fault causes the fault current to flow through the neutrals of all

taps and leads to an inaccuracy in the fault impedance calculation at the relay end because the relay does not receive all the information of the zero–sequence fault current.

The conventional impedance relay falls short when dealing with these problems due to its physical limitations. The introduction of a digital relaying system can provide a solution against the foregoing problems.

1.3 Scope

The purpose of this thesis is to investigate the possible effect of fault resistance carrying current from remote source mainly during the single line–to–ground fault condition, and also the impact on the power system during ground–faults when taps are present. A new adaptive protection scheme will be proposed in this thesis against the shortcomings of the conventional impedance relay under these conditions.

The introductory chapter presents the basic structure of the modern power system as well as the fundamentals of power system protection. The background and advantages of the digital processor based relaying systems have also been given.

The mathematical development of the algorithms in use with the digital relays is discussed in Chapter 2. Then we take a closer look at the theory of Fourier transform analysis.

Chapter 3 discusses the effect of fault resistance carrying remote infeed current during single line–to–ground fault as well as the problems associated with the taps. A new adaptive protection method is presented in this chapter for dealing with these problems.

The simulation results and considerations on the performance of the new protection method are discussed in Chapter 4.

The final chapter is the conclusion.

Background

In the last century, people have learned how to convert certain sources of energy to electricity. Electricity is the only form of energy that can be used for many purposes and is an extremely convenient form of energy for the user. The electric utility industry has been in existence for only hundred years since September 1882, when the world's first electric power in commercial form was sent out from the Pearl Street Generating Station in New York City [1]. The industry has grown over the past hundred years to generate and to deliver electricity.

1.4 Structure of an Electrical Power System

The definition of an electrical power system is given as follows [2]:

An electrical power system is a network of interconnected components designed to convert nonelectrical energy continuously into the electrical form; transport the electrical energy over potentially great distances; transform the electrical energy into a specific form subject to close tolerances, e.g 60 Hz, 120 v.

Typically, the power system can be divided into five subsystems :

Generation	represents the process of converting other nonelectrical forms of energy into electrical energy.
Transmission	of electrical power from generation sites to areas of use through a series of transmission lines. Normally, they are high capacity lines ranging from a hundred MVA to over a thousand MVA.
Subtransmission	via transmission lines with lower capacities and shorter length. When electrical power is brought from the generation sites through transmission lines to a few major stations, it is then transferred to the substations located near the consumer area by the subtransmission lines.
Distribution	system consisting of circuits which extend from the substation to the consumer. There are two basic designs: radial, where power flows in only one direction from the source to load and loop,

where power can flow from more than one direction to the load. In fact, this system is a network. Figure 1.2 [2] shows these two basic designs.

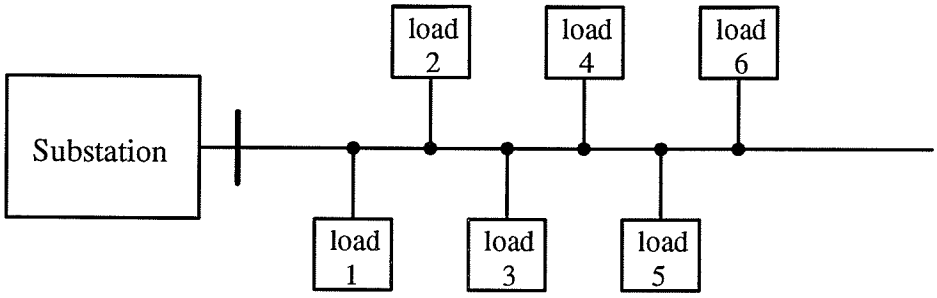

(a)

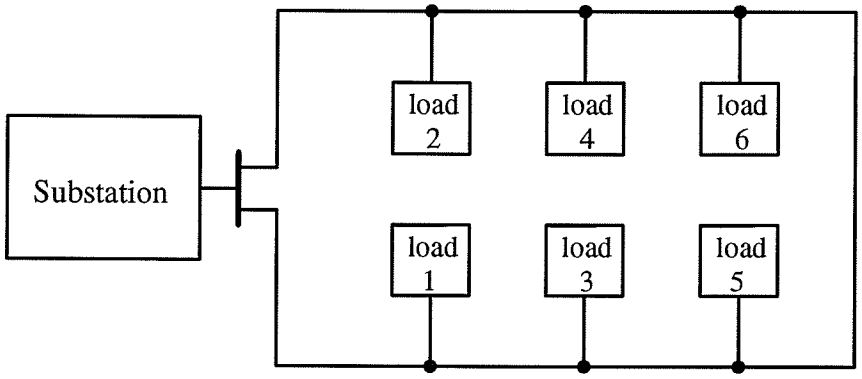

(b)

Figure 1.2 (a) simple radial distribution system. (b) loop distribution system.

Use by numerous devices that consume electrical power. A power system has to deliver the electrical energy to an end user at a suitable voltage level and frequency.

Each of these subsystems can open up its own field of study and discussion, which is beyond the scope of this thesis.

1.5 Power System Protection

An electric power system should ensure the availability of electrical energy without interruption to every load connected to the system. The normal path of the electric current is confined in the metal conductors through generators, transformers and transmission lines to the load. However, there are many chances of these conductors' breakdown due to storms or falling of external objects, so that the current will flow in an abnormal path generally as a short–circuit or "fault". Faults can damage or disrupt power systems in several ways, which may cause loss of revenue due to interruption of service. Therefore, an efficient design of the system protection scheme is needed. The term "protection scheme" is used to describe the whole concept of protecting a power system. An ideal protection scheme should detect and isolate faults instantaneously at any point in the system and accomplish this while keeping as much of the system interconnected as possible. To accomplish this task, some basic protective devices such as instrument transformers, relays and circuit breakers are needed.

It is the function of protective devices known as "relays" to detect abnormal conditions like faults in electrical circuits and operate the correct circuit breakers to isolate faulty equipment from the system as quickly as possible. Since the objective of this thesis is mainly concerned with the relay, the detailed description of the circuit breaker is omitted here. Nevertheless, the function of the instrument transformers will be described in brief in the following subsection.

1.5.1 Instrument Transformers

Detecting abnormal power system operating conditions requires us to monitor power system variables, namely, voltage, current, power, frequency and impedance. Measuring voltage and current enables us to obtain the information of power and impedance, since their relationship is defined as follows:

$$P = |V| \cdot |I| \cos\theta$$

where P is the average power, also called the real power. The cosine of the phase angle θ between the voltage and the current is called the power factor.

The impedance **Z** is defined as:

$$\overline{Z} = \frac{\overline{V}}{\overline{I}}$$

Since power system voltages and currents are at an extremely high level, it is necessary to convert these signals to a lower level for input to a relay. This conversion is necessary for two reasons: 1) the physical hardware of the relay can be small and less expensive for a lower level power input; 2) it provides a safe environment for the relay personnel to work with.

Instrument transformers are commonly used for this purpose. In addition, they insulate the protective equipment from the primary power circuits. Instrument transformers are of two basic types; voltage or potential transformers (PT) and current transformers (CT). The working principle of these instrument transformers is no different from normal transformers, but special attention should be exercised. For example, a current transformer should reproduce the current in its secondary windings from its primary windings as accurately as possible. Similar considerations apply for the voltage transformer. Figure 1.3 [2] shows a typical symbol for PT. $\overline{V}_2$ is the reduced version of $\overline{V}_1$ with no phase shift.

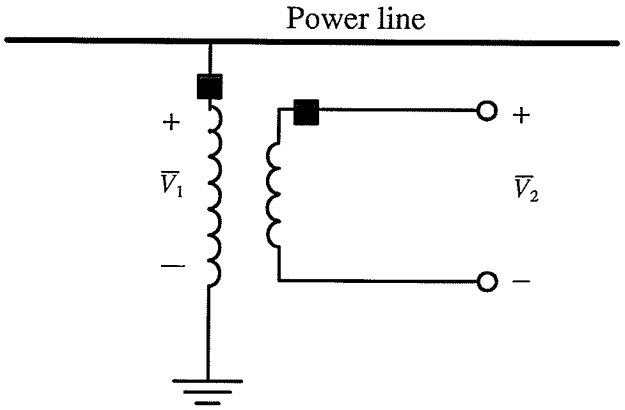

Figure 1.3 Typical symbol for PT.

1.5.2 Relays

In protection schemes, the word "relay" is used to describe the device which measures current, voltage, frequency or impedance. It then isolates the faulty section by controlling the circuit breaker. In general, a relay is expected to sense the change between normal and abnormal conditions and then send an appropriate signal when faults occur. The signal typically energizes the trip coil of its associated circuit breaker which then opens the power circuit. A relay must have the following characteristics:

Reliability — the relay may be sitting idle for most of its lifetime and then be required to operate with fast response. Failure to operate may create a large problem.

Selectivity — the relay should be able to isolate the faulty element of the system and leave the remaining healthy sections intact [3]. The relay should respond only to faults within its own zone.

Sensitivity — the relay should be able to distinguish between a fault and an overload. Abnormal but harmless conditions such as sudden load change or switching transients should not cause mis–operation. It may be noted that the concepts of selectivity and sensitivity can be grouped under the term "security".

Speed — the relay is expected to act as fast as possible. Any prolonged fault situation would result in heavy damage to the power system equipment. Under intentional time delay situations, it must be predictable and adjustable.

There are various types of relays used for system protection. Conventional relays have one of two basic types of construction: (1) electromagnetic or (2) static. In recent years a new type of relay was introduced, which is the digital relay. It will be described in a later section of this chapter.

(1). There are two principal types of electromagnetic relays [5]: (a) attracted armature type; and (b) induction type.

(a) Attracted armature type. This includes plunger, hinged armature type, balanced beam and moving iron polarized relays. All these relays have the same principle; i.e., an electromagnetic force is produced by the operating quantity (induced by fault current).

(b) Induction type. Torque is produced in these relays when one alternating flux reacts with the current induced in the rotor by another alternating flux displaced in time and space but having the same frequency. Depending on whether the rotor is a disc or a cup, the relay is known as either an induction disc or an induction cup relay.

(2). The term "static relay" is generally referred to a relay incorporating solid state components like transistors, diodes, resistors, capacitors, etc [3]. In this type of relay, the functions of comparison and measurement are performed by static circuits wherein there are no moving parts. The output signal operates a tripping device which may be electronic, semiconductor or electromagnetic.

1.5.3 Line Protection

Since a transmission line stretches over a significant geographic area, it is exposed to a variety of hazards such as lightning, wind, ice, birds, etc which cause line faults. An overhead line may experience more faults than other components, so their protective relaying schemes are expected to operate much more frequently. Relays dedicated for line protection can be classified by function, construction or application; e.g. overcurrent relays, directional relays, impedance relays, differential relays and pilot relays.

1.5.3.1 Overcurrent Relays

Overcurrent relays respond to the magnitude of their input current and operate to trip whenever the current magnitude exceeds a pre–set value. It is suitable in situations where fault currents are much greater than load currents. Time delay overcurrent relays are typically used by grading the operating times of successive devices; controlled time delay is important, so that relays may be coordinated properly. It means having relays operate in a sequence so that service is interrupted as little as possible when clearing a fault. To illustrate the point, Figure 1.4 shows a simple radial system. A fault at bus 3 will cause relays at R1, R2, R3 to operate, which then opens all circuit breakers at bus 1, 2, 3. If relay 1 operates before relay 3, bus 2 will be unnecessarily deenergized. Therefore, we need to have a time delay control, so that the relays can operate in a proper sequential order.

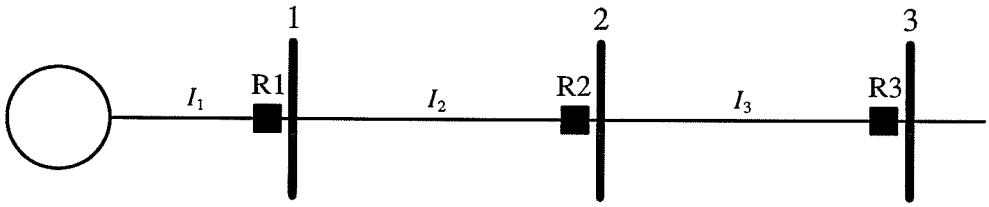

Figure 1.4 A simple overcurrent relay protected radial system.

1.5.3.2 Directional Relays

When the power system becomes complex, time delay control of overcurrent relays becomes quite complicated and in some cases impossible. This problem arises especially in a system with more sources, since the current may be the same in two feeders on the same bus except for its direction. Directional relays can be used to solve this kind of problem.

The working principle of the directional relay utilizes the fact that the impedance of transmission lines is mostly reactive. In such conditions, current should always lag or lead the voltage by an angle of about 90 degrees, and that depends on the direction of the current flow. If the relay can be able to distinguish this difference in phase condition, a directional sensitive relay can be achieved. Figure 1.5 [4] shows a phasor diagram, divided in such a way that for all faults producing current phasors lying in the shaded region the relay will trip, and for all other faults it will block. The boundary of the operating characteristics are defined by angles θ_{min} and θ_{max}. The selectivity of the relay can be adjusted by changing these two angles.

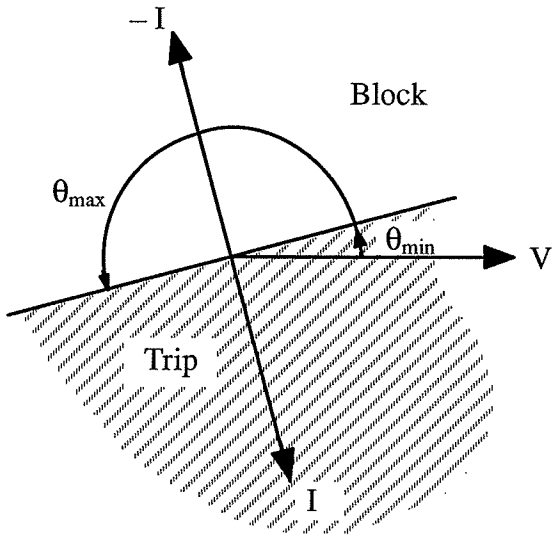

Figure 1.5 Directional relay operating characteristic.

1.5.3.3 Impedance (Distance) Relays

Impedance (Distance) relays recognize faults occurring within the protected section of the transmission line. The distance to the fault is measured in terms of line length. This is done by measuring the voltage to current ratio, which gives the impedance of the transmission line. Since the impedance is proportional to the line length between the relay and the fault it is also a measure of the distance to the fault; hence the term "distance relay".

Consider again the ratio of voltage and current which gives the dimension of the impedance, $\overline{Z} = \overline{V}/\overline{I}$. Under normal conditions, the ratio between voltage and load current would be large, and impedance will have a large magnitude. Under faulted conditions, since the faulted current is much larger than the load current, the ratio Z will be the impedance between the relay and the fault, which is a relatively small number. Therefore, a protective region can be set up where a measured impedance Z is less than a required setting $|Z_r|$. The locus of a constant $|Z_r|$ plotted in the $\overline{Z}$ plane is a circle. The operating characteristic is shown in Figure 1.6a, and it is obvious that this relay is not directional.

It is possible to add directional capability into the distance relay by a simple modification. This is accomplished by offsetting the circle in Figure 1.6b. Such a relay is referred to as a "mho" relay. The circle passing through the origin makes it inherently directional.

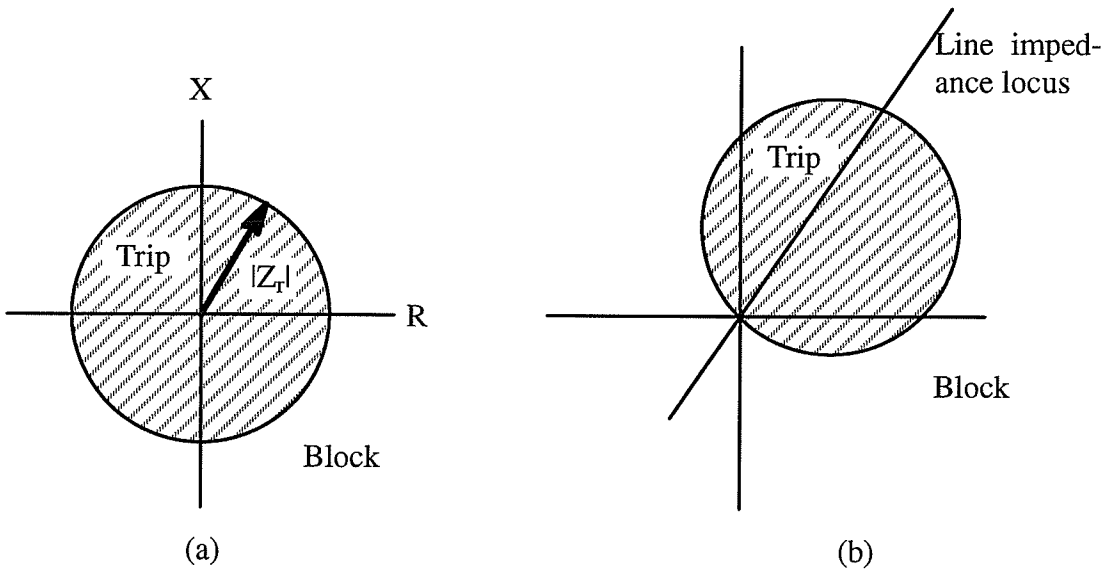

Figure 1.6 Impedance relay characteristic (a) nondirectional relay, (b) mho relay.

In a common protection scheme, there are three distance relays installed per phase with different covered regions respectively. The associated regions are called zones of protection. The relay for zone 1 is typically set for about 80% of the line and

instantaneous operation. Zone 2 and Zone 3 are set for longer reaches and time delay. The objective is to provide a primary and backup protection of the system so that any point in the system will fall within at least two zones of protection.

1.5.3.4 Differential Relays

The principle of operation depends on a simple circulating current. By Kirchoff's law the vector sum of all the currents entering a circuit should be zero unless an additional current path is added (a fault). The relay in this case is a simple comparator which compares magnitude and phase of the currents. To illustrate the point, Figure 1.7 [5], shows a simple differential protection scheme. The secondaries of the current transformers are connected in parallel to the protected equipment and the relay. Under normal conditions, no current should flow in the relay. However, the equilibrium condition would be violated if there is a fault in the protected element which provides an additional current path.

This protection method is not only simple but effective; indeed, it can be made as a very high sensitive relay.

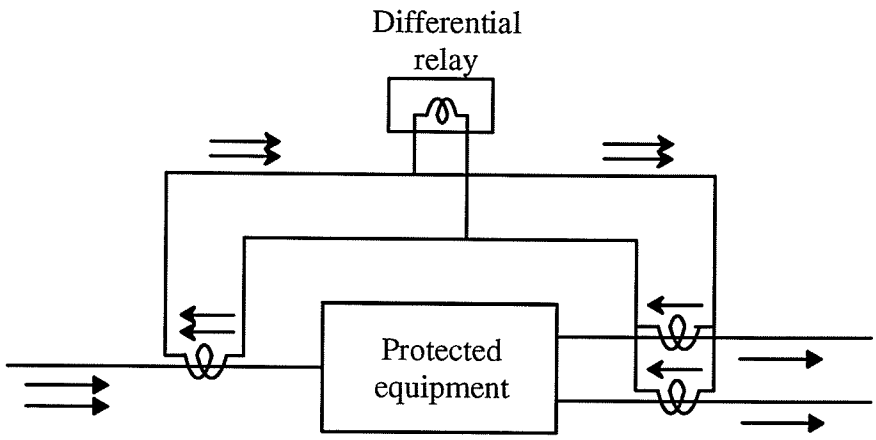

(a) Normal conditions

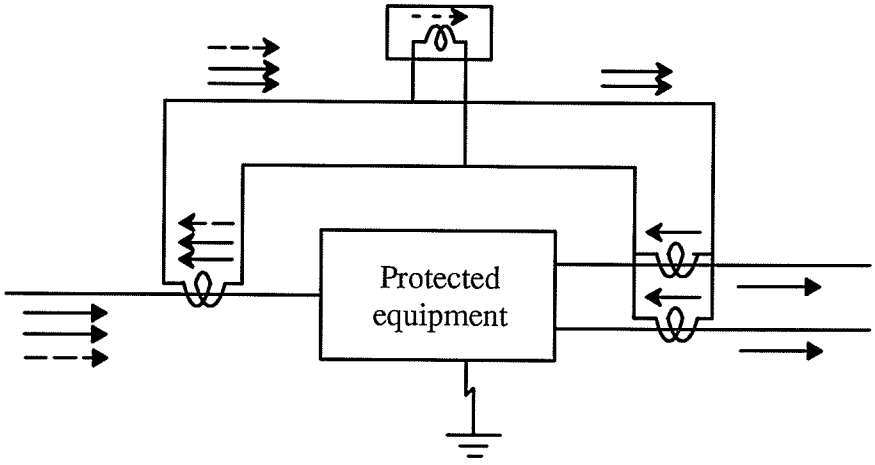

(b) Faulted conditions

Figure 1.7 Differential relay protection scheme

1.5.3.5 Pilot Relays

Pilot relay essentially means remote control of circuit breakers; that is to say, the decision to open or close a local circuit breaker can be made geographically remote from the breaker location. The basic advantage realized is high–speed tripping which permits minimum damage to equipment, minimum stability problems and also automatic reclosing. This scheme requires communication channels to carry system current information to the decision–making location. Three basic channels are used: 1) separate

electrical circuits such as telephone circuits; 2) power line carrier—the power transmission line itself is used as the communication circuit; and 3) microwave – relaying information can be broadcast at microwave frequencies, line of sight, between directional dish antennas. There are several basic pilot relaying schemes in use today, such as a) directional comparison and b) phase comparison scheme.

To illustrate the operation of the pilot protection, consider the simple system shown in Figure 1.8 [4] with fault locations at F1 and F2. The directional relay at B12 cannot distinguish the difference between F1 and F2 (the fault currents both come from the same direction); however, the relay located at B21 sees F1 as an internal fault and F2 as an external fault. Therefore, the relay at B12 will only trip the fault within its own protective zone upon receiving the information from the relay at B21 through the pilot channel. In this way, the need for precise relay settings and corresponding calculated system fault voltages and currents is eliminated. Such a protection scheme is called "directional comparison scheme".

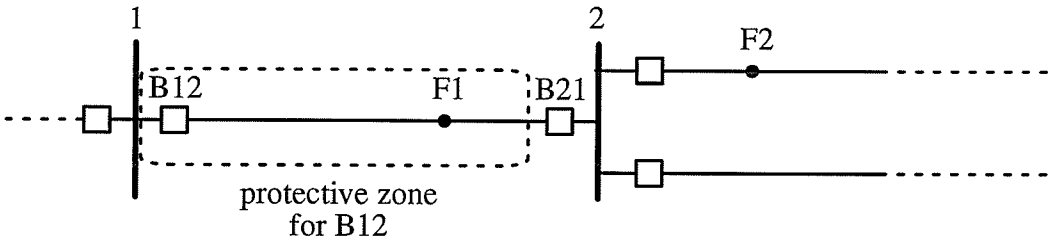

Figure 1.8 Simple "directional comparison" pilot scheme

1.6 Digital Relaying System

Although digital relays possess superior characteristics when compared to their conventional counterparts, it is not until recent years that it has been economically and technically feasible to use them for power system protection. (The early experimental digital relays installed in the mid 70's was about ten times more expensive than the conventional relays they replaced at that time [8]). The dawn of digital relaying systems can perhaps be dated to 1968, the year a paper was written by Rockefeller [6] which described in detail a hypothetical large–scale computer system which is programmed to protect all of the apparatus in and radiating from a major substation. After this paper, many other specific programs and papers were given which helped to develop an experimental mini–computer based system for the protection of a transmission line. Nowadays, many engineers have paid much attention to the use of digital relaying systems. There are definite technical and performance advantages which digital techniques can bring to the relaying art.

The use of a digital technique for protection becomes more important, because it has more advantages than conventional static or electromechanical relays. Among those benefits are :[7]

Flexibility and Adaptive Relaying

With a single, general purpose hardware, the digital relay can be programmed to perform several functions, such as system control and protection. For example, the very same relaying system can be used to respond to different fault conditions with a change of programming only. Therefore, the digital relay can perform tasks such as the relays mentioned in section 1.5.3 with little or no hardware replacement. Besides, faults may only be present for a total of a few seconds out of the relay's 20 or 30 years of service. The idling time of the relaying system can be utilized for monitoring the system load flows, or providing backup for other devices that have failed without any penalty.

The adaptive capability is yet another advantage that is available for the digital relay. This is the ability to change the relay's setting and characteristics depending upon external circumstances. The information for the change can either come from load flow in the protected device or a data link from a central system control. While in some cases the change may be in a specific setting, on the other hand, an all new protection logic function can be selected if needed.

Self Checking Ability

Since the conventional relays are sitting idle for most of their lifetime, even with regular maintenance the reliability for the relays reacting correctly is somewhat doubtful. Digital processors have self–checking ability and most hardware failures can be detected as soon as they occur by a processor stop. Beyond this, specific programs can be used to test the integrity of the relaying system during a non–faulted period.

Cost

While the costs of conventional relays steadily increase, the cost of the digital processor with all peripheral devices for line protection have been declining. With the advance in digital technology, this trend is likely to continue.

Mathematical Capabilities

Digital processors can provide detailed logical and mathematical capabilities. While conventional relay design is constrained by the characteristics and limitations of electromechanical elements or solid state circuits, measurement problems can be stated as digital algorithms and directly implemented in digital relaying systems.

1.6.1 Digital Relay Architecture

Figure 1.9 shows the basic hardware configuration of a digital relay. Although a specific relay may be different in some of its details, a typical digital relay should consist of the components as shown in the figure.

The *Surge Filters* provide an electrical shielding in preventing the damage from the high energy content surges in the analog signals. Normally, these analog signals are the three phase currents and voltages coming from the power system transducers, the conventional ct's and pt's. The analog signals must be low–pass filtered by *Anti–aliasing Filters* before they are sampled, to avoid the effects of aliasing. The effects of aliasing will be described later in Chapter 2. Then the filtered analog signals are converted to digital form by the *Analog to Digital Converter* (ADC). This analog to digital conversion process is called data sampling process. The analog signals are sampled at an even time interval controlled by the *Sampling Clock*, usually between 4 and 32 times per ac cycle (60 Hz). The digital outputs are then fed to the *Processor*. The processor is the central unit in the digital relay which is responsible for the execution of relay programs and makes decisions as to whether there is a fault or not. Moreover, it takes care of the data storage, organization and communication with the external environment. A tripping command can be sent out to the circuit breaker through the *Digital Output* system when a fault is present on the protected line. The *Memory Unit* serves as a reservoir for the storage of the processed data from the processor. It also holds the relay program and other instructions that the processor can load in for execution. The *Communication Channels* can be used to transfer information in and out of the relaying system. The information can be a new relaying setting from other relays or a set of system parameters during fault condition can be sent out to the main control center when needed. Lastly, the *Power Supply* is usually a stand–alone dc battery which is continuously charged by the station power. Under emergency circumstances, this power supply can provide the power to the protection unit.

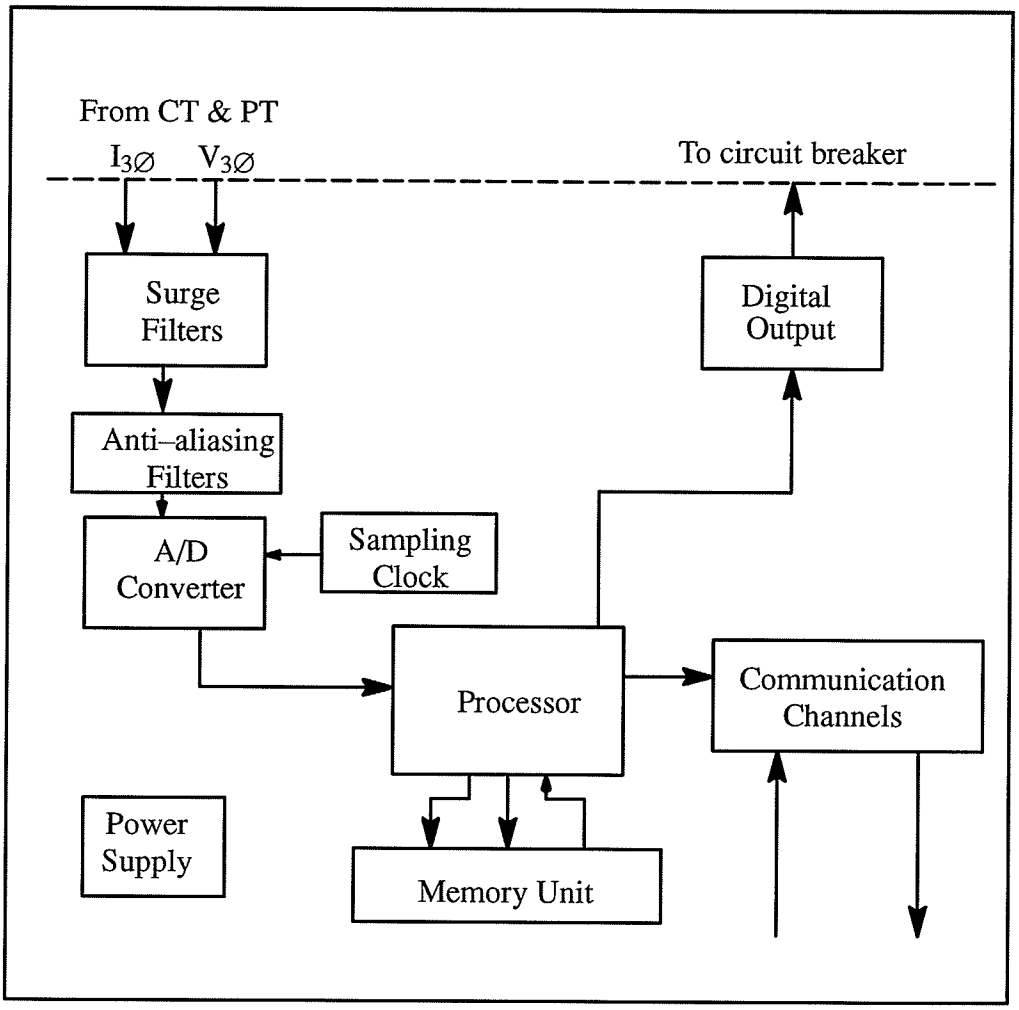

Figure 1.9 A simplified digital relay block diagram

CHAPTER 2

MATHEMATICAL BASIS FOR PROTECTIVE RELAYING ALGORITHMS

In the development of a digital relaying system, despite the continuous progress in the hardware design and configuration, research in the algorithms in use with the digital relay plays a vital role. The algorithms are the programs in the digital relaying system which are responsible for processing the voltage and current samples to produce necessary parameters for protection purposes. Over the past two decades, many researchers have proposed several new and ingenious algorithms, and basically, the currently proposed algorithms can be divided into two groups. The first one is based on a model of the waveforms itself, namely the voltage or current. The algorithms under this category attempt to estimate the fundamental components in order to calculate the impedance to the fault. The following are short descriptions for each algorithm that fits under this group [8] :

1. *Fourier Analysis* [9][10]: This method considers the waveform (voltage or current) as a Fourier Series and performs the Discrete Fourier Transform (DFT) in order to extract the fundamental frequency component from the waveform. Normally, samples are taken over one–cycle period of the signal. It also can be modified to work with a shorter data window for faster response.

2. *Walsh Analysis* [11]: The Walsh Function Algorithm is closely related to the Fourier Analysis. The difference is the use of square waves as the multiplying functions instead of sine and cosine waves in Fourier Analysis. The immediate advantage is the simplification in real–time computation since the values of the reference square waves are ± 1 only. However, a large number of square wave signals are required in order to obtain an accurate estimate of the sinusoidal component.

3. *Curve Fitting Algorithm* [12]: This algorithm is based on the assumption that voltage and current are sinusoidal quantities or even pure sine waves at the fundamental system frequency. The sampled data can be used to calculate resistance and reactance to the fault. Equations for R and X are :

$$X = \frac{v_{n-1}\, i_n - v_n\, i_{n-1}}{(i_{n-1}^2 - i_{n-2}\, i_n)\, \csc\theta} \tag{2.1}$$

$$R = \frac{2\, v_{n-1}\, i_{n-1} - v_n\, i_{n-1} - v_{n-2}\, i_n}{2\, (i_{n-1}^2 - i_{n-2}\, i_n)} \tag{2.2}$$

where θ is the fundamental frequency angle between samples.

Since the equations only use three consecutive samples, the algorithm is ideal for situations when fast response is needed. However, it is highly vulnerable to dc offsets and harmonic contamination.

4. *Derivative Calculation* [13]: There are two algorithms that utilize the idea of derivative calculation, 1). Sample and Derivative Calculation, and 2). First and Second Derivative Calculation. They both take the differentiation of the assumed fundamental waveform ($v = V \sin(\omega t + \theta)$) to obtain the desired peak value or phase of the estimated component.

The equations used in the first method are :

$$| V | = \sqrt{(v_k)^2 + (v_k')^2} \tag{2.3}$$

$$\theta_v = \arctan\left[\frac{v_k}{v_k'}\right] \tag{2.4}$$

where $v_k' = \frac{1}{\Delta t \omega}[v_{k+1} - v_{k-1}]$

Δt = the time interval between samples.

ω = the fundamental power system frequency in radians per second.

Despite the fact that this algorithm gives an excellent response to the sudden change in the waveform, it suffers from the deterioration caused by dc offset, harmonics, and other high frequencies.

The equations used in First and Second Derivative Calculation are :

$$V = (v_k') + (v_k'') \tag{2.5}$$

$$\theta_V = -\arctan\frac{v_k''}{v_k'} \tag{2.6}$$

where $v_k'' = \frac{1}{\Delta t\omega}(v_{k+1} - 2v_k + v_{k-1})$

The advantage of this algorithm is its immunity from the effect of dc offset since the constant dc term is deleted from all the differentiated expressions. Nevertheless, the use of first and second derivatives may introduce even bigger errors than in the Sample and First Derivative Calculation when dealing with harmonics and high frequencies.

Viewing the problem in a different way, the second type of parameter estimation is based on a model of the system rather than the waveforms. The representation in this category is the *Differential–Equation Algorithms* [14]. It considers the transmission line being protected as a simple R–L lumped parameter circuit. The differential equation describing that model is :

$$v(t) = R\, i(t) + L\frac{di(t)}{dt} \tag{2.7}$$

Since v(t) and i(t) are measured quantities, equation yields R and L values directly and hence the distance from the relaying point to the fault. Dc offsets in this case do not cause errors because they are now a valid component of the fault currents. However, they are limited in their usefulness when system structure at the source bus becomes complicated [7].

2.1 Fourier Analysis

All the algorithms mentioned in the previous section have their advantages and disadvantages according to the assumptions they are based on. Nevertheless, the Fourier Analysis offers more desirable benefits than the others in terms of simplicity and performance. The usefulness of the Fourier Analysis is already well–known in the communication study [15]. There even exists many Digital Signal Processors (DSP) which perform *Fast Fourier Transform* (FFT) with their built–in function. All these factors make utilization of the Fourier Analysis to extract the fundamental components very attractive, and it is well worth a closer look at the theory behind it.

2.1.1 Fourier Series

Since the same mathematical technique can be applied for either voltage or current waveforms, for generality, waveforms will be denoted simply as w(t).

A waveform w(t) is periodic with period T_o if

$$w(t) = w(t + T_o) \tag{2.8}$$

where T_o is the smallest positive number that satisfies this relationship. This period T_o is also called the fundamental period of w(t). Then, a sinusoidal waveform of fundamental frequency $\omega_o = \frac{2\pi}{T_o}$ is periodic since it satisfies (2.8).

The periodic waveform w(t) can be represented over the interval $a < t < a+T_o$ by the *Fourier series*

$$w(t) = \sum_{n=-\infty}^{n=\infty} c_n \, e^{jn\omega_o t} \tag{2.9}$$

where the Fourier coefficients c_n are given by

$$c_n = \frac{1}{T_o}\int_a^{a+T_o} w(t)e^{-jn\omega_o t}dt \qquad (2.10)$$

Since the waveform *w(t)* is periodic with period T_o, this Fourier series is therefore valid over all time, $-\infty < t < \infty$. From (2.9), when n = 1 the corresponding frequency $f_o = 1/T_o$ is said to be the fundamental frequency and frequency nf_o is representing the nth harmonics frequency, where n > 1. The Fourier coefficient c_o is equivalent to the dc value of the waveform *w(t)*. Hence, a full representation of each composition (dc value, fundamental component, harmonics) within the waveform (voltage or current) can be achieved.

2.1.2 Fourier Transform

When a particular frequency component is to be examined, one needs to view the waveform over all time to be sure that the measurement is accurate. The relative level of one frequency as compared to another is given by the frequency spectrum. This is obtained by taking the *Fourier transform* of the waveform. The Fourier transform of a waveform w(t) is given by :

$$W(\omega) = \int_{-\infty}^{\infty} w(t)\ e^{-j\omega t}\ dt \qquad (2.11)$$

From (2.11), it is obvious that the spectrum of the waveform is obtained only by a mathematical calculation. By definition, the waveform is observed over the infinite time interval $(-\infty, \infty)$, which is physically impossible. However, a relatively simple and effective approximation of (2.11) can be acquired by using the *discrete Fourier transform* (DFT), which is :

$$X(n\Omega_o) = \sum_{k=0}^{k=N-1} x(k\tau)\ e^{-jn\omega k\tau} \qquad (2.12)$$

where N = number of samples taken over one period.

T = sampling period.

τ = T/N, the sampling interval.

ω = $2\pi / T$, the angular frequency.

n = the harmonic order.

Ω_o = $2\pi / NT$, fundamental frequency of discrete samples.

The approximation is obtained by taking N samples of the continuous waveforms w(t) at intervals of τ seconds over the period of T sec. If N is large enough, w(t) can be represented by this discrete–time signal x(k) as shown in Figure 2.1 [7]. Then the transform of x(k) gives a finite description of the transform of w(t). Given the number of *n*, the waveform component at that particular frequency can be obtained. The restriction is that for *N* samples per cycles, the maximum harmonic order which can be obtained is the $(\frac{N}{2} - 1)$ th.

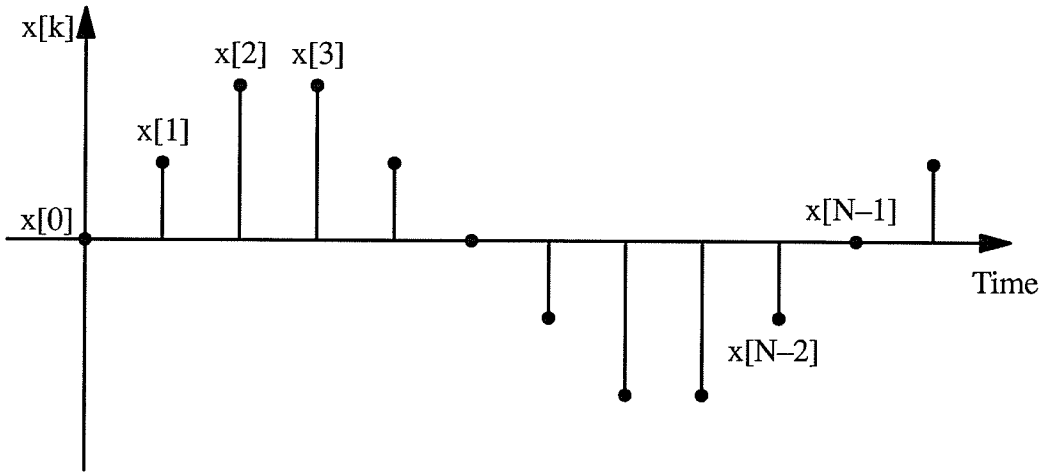

Figure 2.1 The sampled data

2.1.3 Fast Fourier Transform

The Fast Fourier Transform (FFT) is not a new type of transformation, but rather it represents a means for computing the DFT with a considerable reduction in the number of calculations. The FFT also allows a more accurate computation of the DFT by reducing roundoff errors. Nowadays many DSP chips have the FFT function built–in which makes them the essential components in the digital relaying system.

Instead of presenting a thorough development of the analytical theory of the FFT, a somewhat simplified overall discussion of the general idea of the FFT is presented here.

Consider the expression of the DFT in eqn. (2.12) [16], if we rewrite it as follows :

$$X_n = \sum_{k=0}^{k=N-1} x_k \, e^{-j(2\pi nk/N)} \tag{2.13}$$

where $x_k = x(k\tau)$

$X_n = X(n\Omega_o)$

and $n = 0, 1, \ldots, N-1$

To simplify the notation of (2.13), let W represent the invariant part of the exponential term, so that

$$W = e^{-j2\pi/N} \tag{2.14}$$

and now, eqn. (2.13) becomes

$$X_n = \sum_{k=0}^{N-1} x_k \, W^{nk} \tag{2.15}$$

The above expression can be expressed in a matrix form as :

$$\begin{bmatrix} X_0 \\ X_1 \\ X_2 \\ . \\ . \\ . \\ X_{N-1} \end{bmatrix} = \begin{bmatrix} 1 & 1 & 1 & 1 & .. & 1 \\ 1 & W & W^2 & W^3 & .. & W^{N-1} \\ 1 & W^2 & W^4 & W^6 & .. & W^{2(N-1)} \\ . & . & . & & & . \\ . & . & . & & & . \\ . & . & . & & & . \\ 1 & W^{(N-1)} & W^{2(N-1)} & & & W^{(N-1)(N-1)} \end{bmatrix} \begin{bmatrix} x_o \\ x_1 \\ x_2 \\ . \\ . \\ . \\ x_{N-1} \end{bmatrix} \qquad (2.16)$$

The above square matrix with order N can be factored into several subsets where each of these subsets has only a few non–zero elements in their rows. Therefore, a significant reduction in computation can be achieved under this condition. While it is possible to develop the FFT that works with any number of samples per cycle, a simple and particularly effective computation is achieved when N is a power of 2; i.e. 2^y where y is any positive integer.

A simple measure of the amount of computation in the DFT reveals that about N^2 products in computation are required for the set $[X_n]$ whereas the number of computations for the FFT is about $N \log_2 N$. The approximate ratio of the computation steps between the DFT and the FFT is given in the following table.

N	N(DFT)	N(FFT)	N(FFT)/N(DFT)
16	256	64	0.250
32	1024	160	0.156
64	4096	384	0.0938

Table 2–1 Comparison of number of computations between DFT and FFT

The DFT uses less computation steps only when just one particular frequency term is needed and where N is small. There is still little reason to use the DFT since the saving in the computation time in comparison to the FFT is small. Moreover, the FFT is

capable of giving the real and imaginary parts for all harmonics up to the $(\frac{N}{2} - 1)$ th term while the DFT only gives the output at one particular harmonic order. Therefore, for $N = 32$ samples per cycle, up to the 15 th harmonic term can be obtained.

Perhaps most relay engineers are not familiar with the use of the Fourier Transform since most of the works are under the field of communication study. There is no book specially directed towards the theory of this subject under the power system protection category. Nevertheless, several excellent books which give an explanation of the Fourier Transform under the communication study field are included in the Bibliography.

2.1.4 Effect of aliasing

In addition, when using the Fourier Transform, the aliasing effect during waveform sampling should be avoided since it introduces errors in the transform process. It is known that the spectrum of a sampled waveform consists of shifted replicas of $X(\omega)$ at the harmonics of the sampling frequency f_s as shown in figure 2.2 [15]. If $f_s < 2B$, where B is the highest significant frequency component in the original waveform, the shifted replicas will overlap with each other as shown in Figure 2.3. This spectral overlap is called aliasing. In order to avoid aliasing, an anti–aliasing filter can be used. The anti–aliasing filter is a low–pass filter which physically filters out the frequency components above $|f| = f_s / 2$ before sampling.

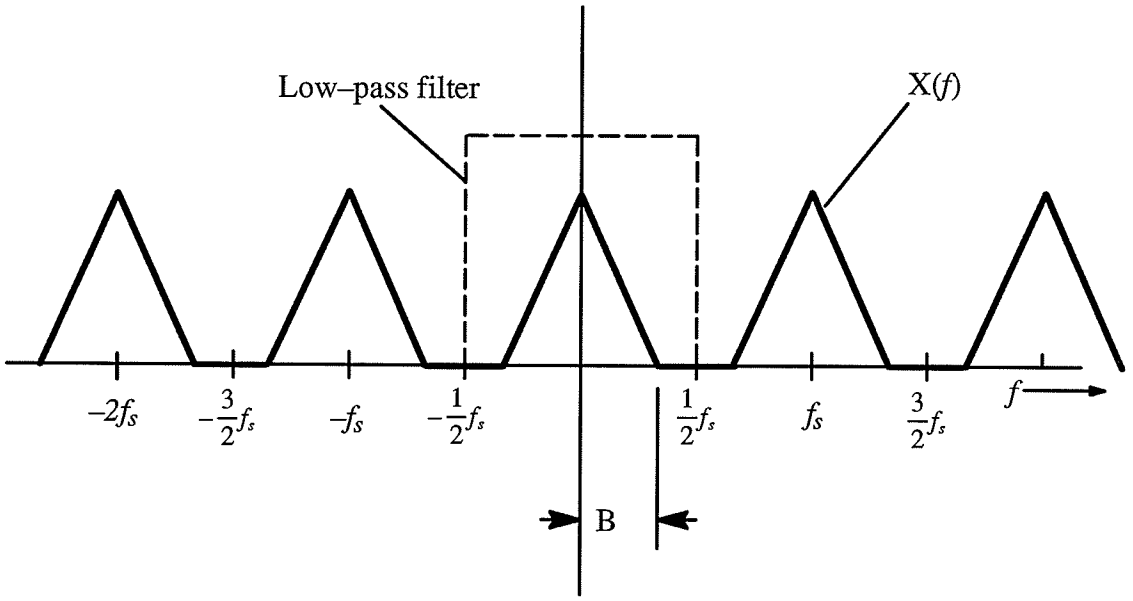

Figure 2.2 Spectrum of sampled waveform ($f_s > 2B$)

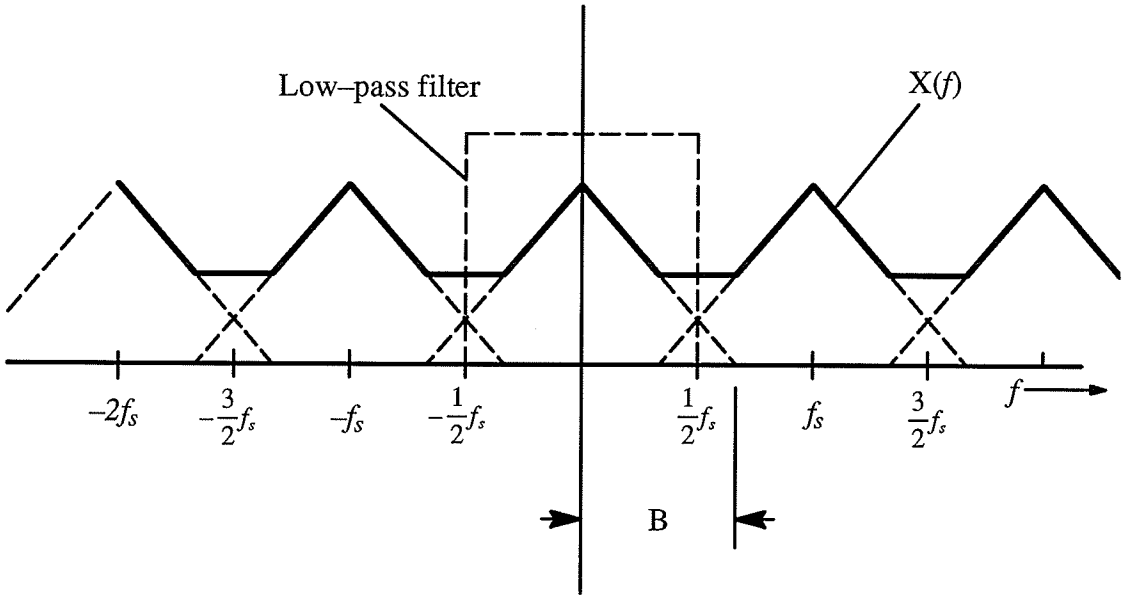

Figure 2.3 Spectrum of sampled waveform ($f_s < 2B$)

2.2 Symmetrical Components

The power system normally operates in a balanced three–phase steady–state mode. However, with unbalanced faults, such as single–line to ground fault, or line to

line fault, the conditions in all the phases are obviously not the same. The fault calculation for each phase separately will be complicated and troublesome. The use of symmetrical components provides a much quicker and simpler way to deal with the above problem.

Symmetrical components were introduced by Dr. Fortescue in 1918 [17] and even today are among the most powerful tools of analysis available to a power system engineer. Many papers have been published on the use of symmetrical components in the field of relaying and protection [18][19].

CHAPTER 3

EFFECT OF SINGLE–PHASE TO GROUND FAULT RESISTANCE ON SYSTEM WITH OR WITHOUT TAPS

With all the different relays described earlier, overcurrent relays and impedance relays are most commonly used for the protection of transmission lines. Overcurrent relays with the directional capability are usually used to protect the short radial or simple loop transmission line systems. In a high–voltage (HV) or extra–high voltage (EHV) system there are possibly many generating stations and subtransmission feed points interconnected to form a network. The complexity of the system makes the simple current level detector such as the overcurrent relay inadequate for providing an accurate fault reading. Conventional impedance relays use phase or amplitude comparators to decide whether the $\frac{\overline{V}}{\overline{I}}$ ratio falls within a predetermined trip boundary and do not depend upon the fault current levels. Therefore, impedance relays are among the most desirable protection devices in many transmission line protection applications.

3.1 Background

A typical single–line diagram of a power system with ground fault is shown in figure 3.1. The system with a source of power at each end of the line and other elements on the transmission line is shown in detail in the figure. A single line–to–ground fault is assumed to occur between phase a and the ground at point F, a fraction m of the total distance L from bus A to bus B. Since the line impedance is proportional to the distance, the impedance from A to F becomes mZ_L and from F to B becomes $(1-m)Z_L$. The impedance relay located at bus A monitors the voltage phasor and current phasor to determine the value of the fault impedance. This fault impedance is a complex quantity consisting mainly of inductive reactance with a relatively small resistance. Since the measured impedance is proportional to the distance to the fault, the impedance relay also

provides an indication of the general area where the fault occurred, and a fault locator can be implemented based on this information.

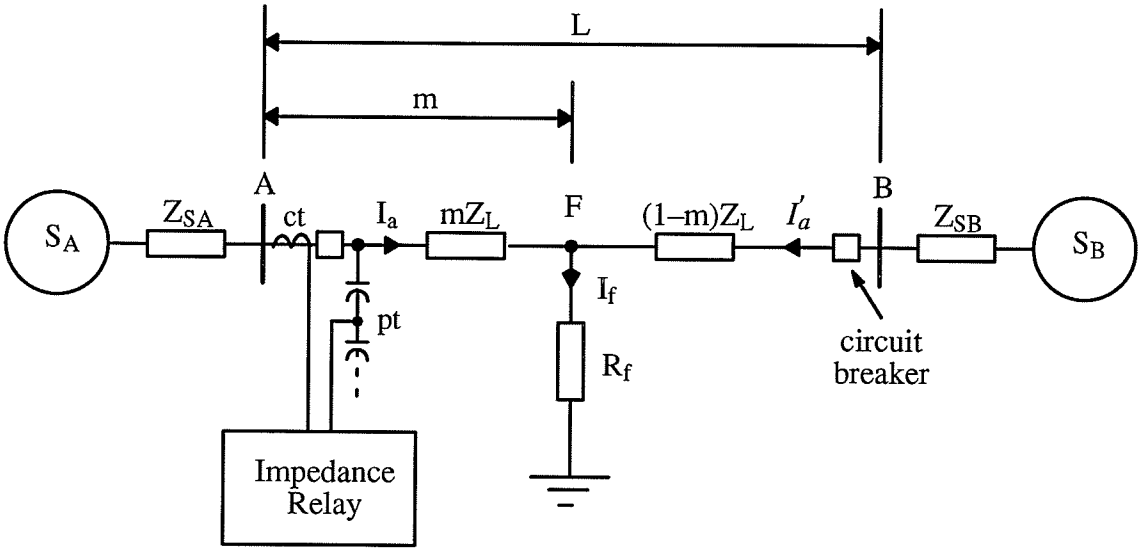

Figure 3.1 Power system single–line diagram with ground fault

Rather than using the simple $\frac{\overline{V}}{\overline{I}}$ ratio to determine the impedance value of a single–line to ground fault, Lewis and Tippett in their classical paper [20] presented the following fundamental equation for this specific type of fault :

$$Z_m = \frac{E_a}{I_a + KI_0} \tag{3.1}$$

where Z_m = Measured impedance at the relay end.

E_a = Line to ground voltage measured at the relay end with phase *a* as the faulted phase.

I_a = Phase A current measured at the relay end.

$K = \frac{Z_{0L} - Z_{1L}}{Z_{1L}}$, Z_{0L} is the zero–sequence line impedance and Z_{1L} is the positive–sequence line impedance.

I_0 = Zero–sequence current measured at the relay end.

In order to understand why the use of eqn. (3.1) is superior to the simple $\frac{\overline{V}}{\overline{I}}$ ratio, determination of fault voltages and currents using the symmetrical components method is required. The corresponding sequence impedance networks for the power system in figure 3.1 are set up and shown in figure 3.2. The positive sequence network is given in Figure 3.2a with E and E' to represent the equivalent line–to–neutral voltage source at S_A and S_B respectively. The negative–sequence network is given in figure 3.2b. In this network there is no voltage source and the impedance is equal to the one in the positive–sequence network. Nevertheless, distinct subscripts are maintained for keeping the two networks distinct.

The actual calculation of the faulted voltages is included in Appendix I. Eqn. (A.6) from Appendix I gives the calculated voltage E_a which is shown here in eqn. (3.2). If the faulted line current I_a is used for the tripping signal in conjunction with the voltage E_a, the measured impedance at the relay point is given in eqn. (3.3).

$$E_a = I_a(mZ_{1L} + R_f) + I_a'R_f + I_0m(Z_{0L} - Z_{1L}) \tag{3.2}$$

$$Z_m = mZ_{1L} + R_f + \frac{I_a'}{I_a}R_f + \frac{I_0}{I_a}m(Z_{0L} - Z_{1L}) \tag{3.3}$$

It is obvious that the quantity Z_m is affected by the value of the fault resistance R_f, the ratio between the fault phase current from the remote end and the source end, and also by the zero–sequence current in the line being protected. As the individual magnitude of R_f and I_a' are unmeasurable at the location of the relay, it causes difficulty in some situations. Moreover, the variable term $\frac{I_0}{I_a}m(Z_{0L} - Z_{1L})$ is another source of error in calculating the fault impedance. According to the information in ref. [20], the

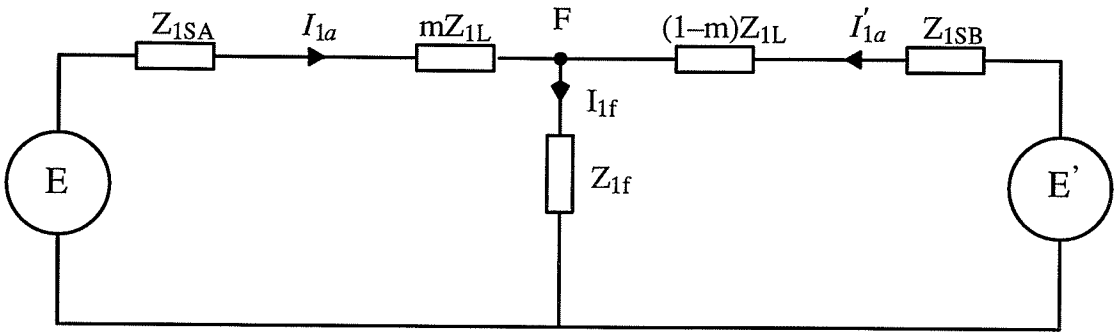

(a) Positive–sequence network

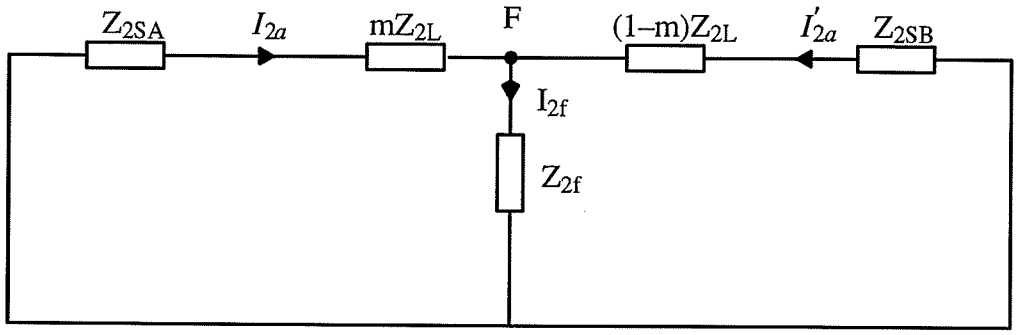

(b) Negative–sequence network

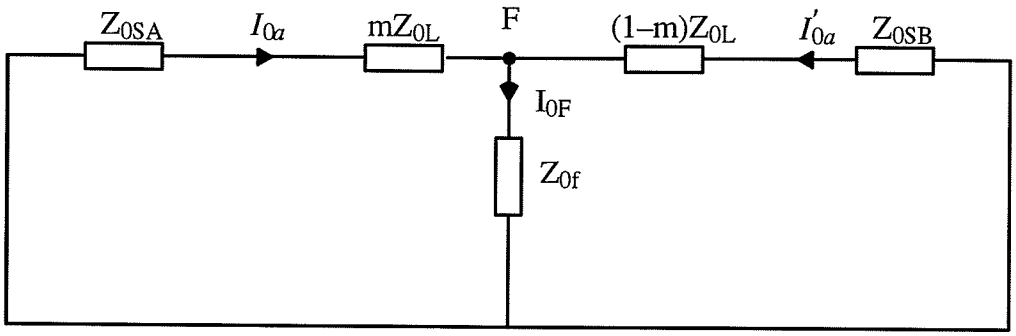

(c) Zero–sequence network

Figure 3.2 Sequence impedance networks

ratio $\frac{I_0}{I_a}$ is not fixed at the value one third unless there is only one path for the fault to flow. From figure 3.1, it is obvious that the fault current is not coming from only source A but also from the remote end B. The condition of the fault current fed from only one end can be achieved after the circuit breaker at busbar B has opened. The $\frac{I_0}{I_a}$ ratio varies over a range depending upon the location of the fault. Under the condition where the fault current is fed from both ends, the ratio will be less than one third when the fault takes place near the remote protected boundary. The ratio then falls back to one third after the circuit breaker at B is open. This breaker opening action causes an increase in impedance which may lead to the relay's underreach [20].

From what has preceded, it is evident that the performance of the relay using the $\frac{\overline{V}}{\overline{I}}$ ratio as the tripping signal is not entirely satisfactory. Therefore, an improvement must be sought. As the currents and voltages are the main or perhaps the only information available for the protective relay, they may be modified to give a more acceptable result. Referring to eqn. (A.11) in Appendix I, the voltage E_a may once again be written in a different form by factoring mZ_{1L} out of all terms and obtain :

$$E_a = (I_1 + I_2 + I_0)mZ_{1L} + (\frac{Z_{0L}}{Z_{1L}} - 1)I_0 mZ_{1L} + 3(I_0 + I_0')R_f \tag{3.4}$$

$$= [I_a + (\frac{Z_{0L}}{Z_{1L}} - 1)I_0]mZ_{1L} + 3(I_0 + I_0')R_f \tag{3.5}$$

If we let

$$K = (\frac{Z_{0L}}{Z_{1L}} - 1) \tag{3.6}$$

and let I_r be the divisor of eqn. (3.5) where I_r is defined by the equation

$$I_r = I_a + KI_0 \tag{3.7}$$

Now we have the result which is the same as the one in eqn. (3.1) and it can be written in a different way as follows :

$$Z_m = mZ_{1L} + \frac{3(I_0 + I_0')}{I_r} R_f \tag{3.8}$$

It is evident immediately that the $\frac{I_0}{I_a}$ ratio which was causing difficulty in the first place is omitted in this new expression. The first term of eqn. (3.8) is directly proportional to the distance from the relay to the fault and the second term is a function of the fault resistance R_f. The term $[(I_0 + I_0') / I_r]$ gives a pure resistance effect if the dividend and the divisor have their phase angle in a close proximity to each other. In general, all the impedances in eqn. (3.8) will have a very close phase angle, unless the line resistance is very large; hence, the line current I_a and zero–sequence currents I_0, I_0' should be nearly in phase.

When comparing eqn. (3.3) and eqn. (3.8), both fault impedance expressions suffer from the unknown of remote infeed current data. However, all things being equal, the new expression does indeed have an improved performance over the original one.

3.2 Effect of ground fault resistance and remote infeed

In the preceding discussion, the fault resistance R_f was mentioned and is one of the unknown quantities in calculating the fault impedance at the relaying point. In a realistic situation, the ground fault is seldom a perfect short, but rather an impedance with relatively high resistance. Consider the fault resistance term included in eqn. (3.8). The fault currents $(I_0 + I_0')$ and I_r were assumed to be in phase in the previous

discussion. However, under the influence of the fault resistance it may not be true, and the remote source infeeds to the fault branch may significantly modify the apparent impedance presented to the relay. A more precise expression should be included with the phase angle term and which is shown as follows :

$$Z_m = mZ_{1L} + \left|\frac{3(I_0 + I_0')}{I_r}\right| R_f \cdot e^{j\frac{(I_0 + I_0')}{I_r}} \qquad (3.9)$$

The fault current from both local and remote terminals causes a voltage drop in the fault branch and if it is not in phase with the local fault current, it gives a reactance effect and shifts the fault locus up or down in the R–X plane as well as to the right. In general, the shift direction and magnitude for the fault locus is dependent upon the system power flow at the time of the fault. This may lead to two possible situations :

(a) where fault takes place beyond the protected boundary it may possibly drop within the relay operating zone to cause mal–operation.

(b) where fault takes place within the protected boundary it may possibly drop out of the relay operating zone to cause failure to trip.

For illustration, Figure 3.3 shows an impedance relay's quadrilateral type characteristics boundary **XPRO** in the R–X plane.

In the case when the power sources at both ends are in phase (no real power flow), the voltage and current in the fault branch will be in phase and produce a pure resistance effect which shifts the apparent impedance to the right as shown in Figure 3.3. If the tripping characteristic has a large resistive reach like the one in Figure 3.3, the magnified fault resistance can therefore be tolerated.

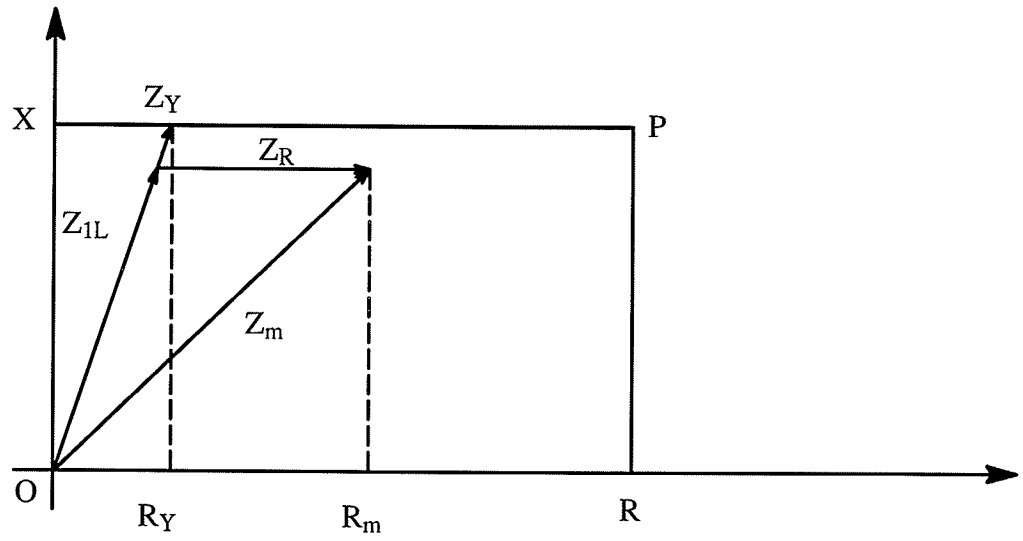

Figure 3.3 Trip characteristic with ground fault resistance (no real power flow)

In the case when the local source is leading the remote source (power flow out of the relay location), the fault voltage will lag the current in the fault branch and shift the fault impedance locus downward through an angle α as shown in Figure 3.4. This causes a possible overreach error.

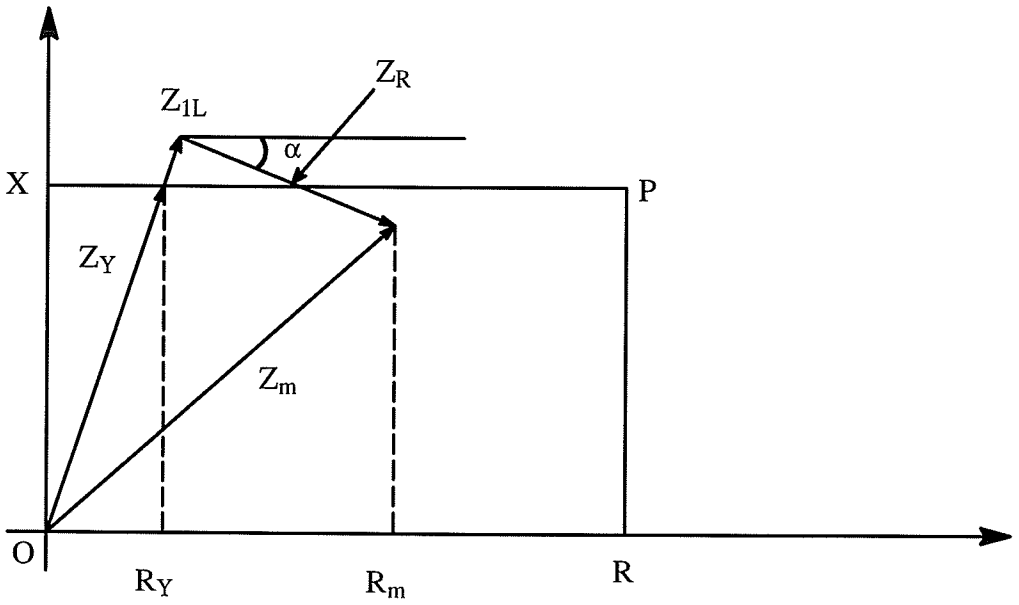

Figure 3.4 Trip characteristic with ground fault resistance (power output)

In the case when the local source is lagging the remote source (power flow into the relay location), the fault voltage will lead the current in the fault branch and shift the fault impedance locus upward through an angle α as shown in Figure 3.5. This causes a possible underreach error.

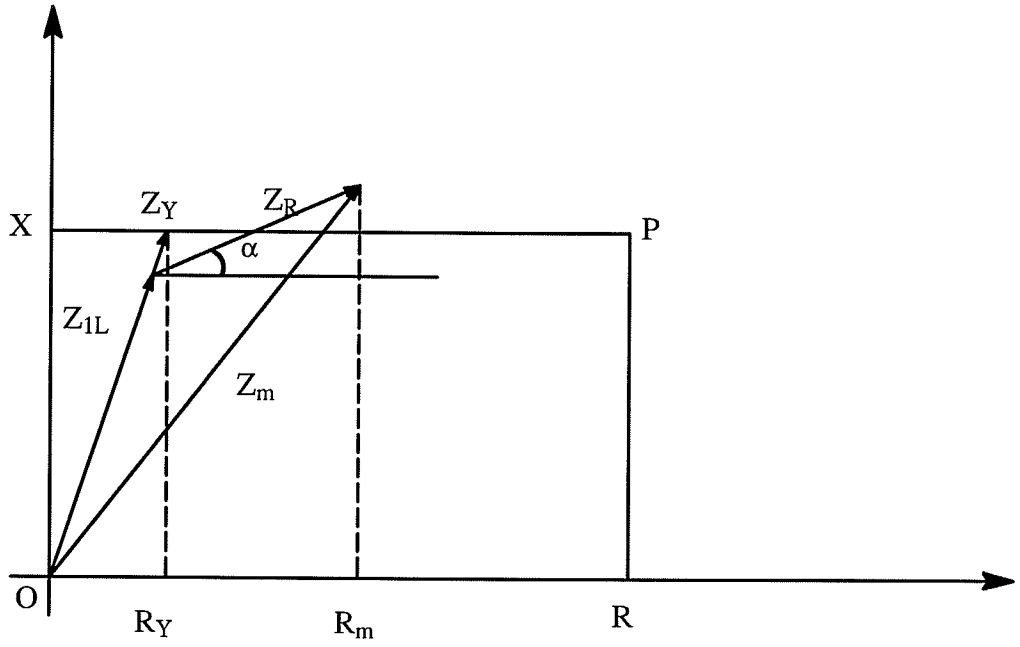

Figure 3.5 Trip characteristic with ground fault resistance (power input)

3.3 Adaptive relay with improved coverage for fault resistance and remote infeed

In order to remedy the errors caused by the ground fault resistance and remote infeed, a new adaptive method for single line–to–ground fault protection is suggested here [21]. It is believed that this adaptive method can provide the digital impedance relay the ability to automatically adjust its operating boundary so as to more closely follow the locus of the measured impedance associated with various prefault load flow conditions.

Considering Figure 3.4 and Figure 3.5, if the operating characteristic boundary **XP** of the impedance relay can be rotated through the same angle as angle α around a reference point as center, then the characteristic boundary **XPRO** will be changed into a

new quadrilateral **X'P'RO**, as shown in Figure 3.6 and Figure 3.7 correspondingly. The logical center point chosen here is point Y at the line impedance locus. In this way, the maloperation of the protective relay can be avoided and the elimination of the disadvantageous influence of the fault resistance is feasible.

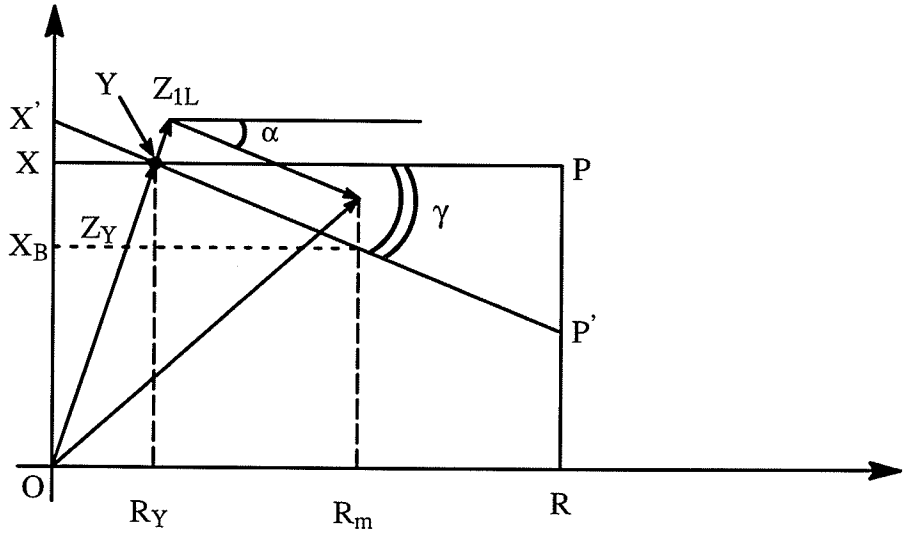

Figure 3.6 Adaptively changed trip characteristic (power output)

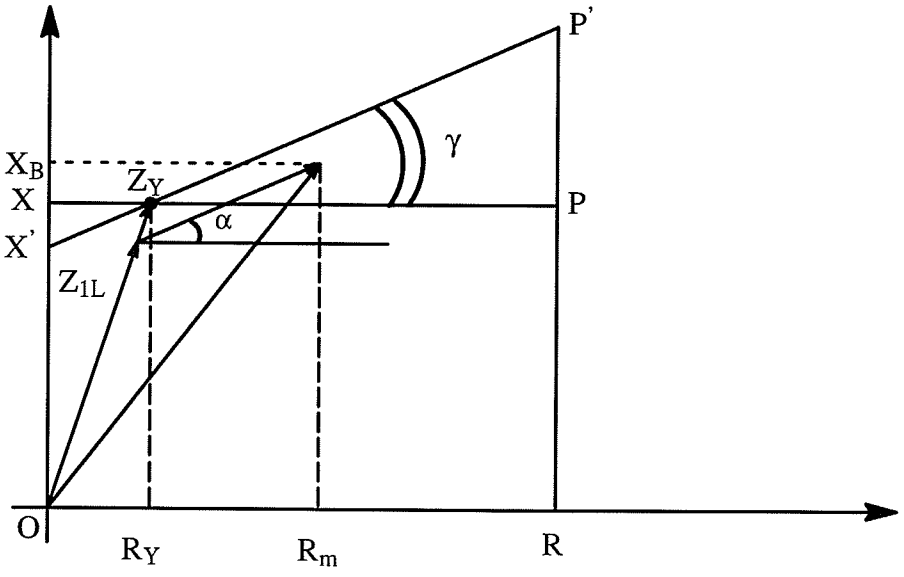

Figure 3.7 Adaptively changed trip characteristic (power input)

From eqn. (3.9) on page 36, we know that

$$\alpha = \angle[(I_0 + I_0') / (I_a + KI_0)] \tag{3.10}$$

For analysis purposes, we need to derive the relationship between angle α and the fault impedance presented to the impedance relay. The mathematical development is included in Appendix II. It has been shown in eqn. (A.17) of Appendix II that the impedance at the relaying point with fault resistance R_f is given by :

$$Z_m \simeq mZ_{1L} + \frac{I_0(Z_{0SA} + Z_{0L} + Z_{0SB})3R_f}{(I_a + KI_0)[(1-m)Z_{0L} + Z_{0SB}]} \tag{3.11}$$

$$\simeq mZ_{1L} + R_f' \angle\alpha$$

It is obvious that the unmeasurable remote infeed data I_0' is omitted in the above expression and is replaced by impedance terms. Now, the expression for angle α can be written in a different form :

$$\alpha = \angle I_0 / (I_a + KI_0) + \angle(Z_{0SA} + Z_{0L} + Z_{0SB}) / [(1-m)Z_{0L} + Z_{0SB}] \tag{3.12}$$

If the magnitude of angle α can be measured at the relaying point, a perfect compensation for the effect of remote infeeds is achieved by rotating the characteristic boundary XP through the same angle as α. However, the perfect compensation is rarely achieved because not all fault information is available for the protective relay. There exists a component in the variable α which can not be obtained conveniently at the time of fault. If we let

$$\theta = \angle(Z_{0SA} + Z_{0L} + Z_{0SB}) / [(1-m)Z_{0L} + Z_{0SB}] \tag{3.13}$$

$$\beta = \angle I_0 / (I_a + KI_0) \tag{3.14}$$

Then

$$\alpha = \beta + \theta$$

With reference to eqn. (3.13), it is evident that the magnitude of θ is dependent on the zero–sequence impedances of the line being protected and the sources at both ends, and on the fault location. The magnitude of θ is not available to the relay since the location of the fault is still an unknown prior to the fault calculation. The only information which is accessible at the relaying point is angle β. Therefore, the difference between angle β and angle α is an important factor which determines the effect of remote infeeds on accuracy during fault resistance with remote infeed conditions. Although the value of θ is dependent upon the fault location along the line, its value only varies slightly for fault occurring near the remote boundary. Nevertheless, for the sake of improving the accuracy of the impedance relay near the remote boundary, the value of θ can be calculated beforehand since the only unknown in eqn. (3.13) is "m" which is the fraction of the total line length from the relay to the location of the fault. For a remote boundary set at 80% of the total line length, the value of m is simply 0.8; hence the value of θ can be calculated. Assuming θ_Y is the value of such a θ located at the remote boundary, then, a new expression is introduced, which is :

$$\gamma = \beta + \theta_Y \qquad (3.15)$$

A comparison between α and γ shows that the only difference comes from the latter term θ. When a fault occurs near the remote boundary, θ should be approximately equal to the predetermined value θ_Y, and thus γ should be approximately equal to α also. Therefore, instead of using angle α as the rotation reference, it is replaced by γ and the boundary **XP** rotates through such an angle to become **X'P'** as shown in Figure 3.6 and Figure 3.7. After such boundary manipulation, the tolerance to

the fault resistance with remote infeed for the impedance relay is effectively increased and the accuracy for the impedance relay's protection near the remote boundary can be improved.

3.3.1 The procedure for applying the adaptive protection method

For the adaptive method described in the previous section, it is easily implemented on a protective system equipped with the digital relay. The measured quantities of the digital relay are commonly in phasor forms such as the voltage phasor (a, b) and current phasor (c, d). From this phasor value, the fault impedance can be evaluated very easily by [22]:

$$R = \frac{ac + bd}{c^2 + d^2} \quad , \quad X = \frac{ad - bc}{c^2 + d^2} \tag{3.16}$$

In the case when dealing with the single line–to–ground fault, the current phasor is replaced by the residual compensated current phasor I_{AL}, which equal to I_a+KI_0 where the reason has already been discussed in section 3.1.

The procedure for applying the adaptive protection method is as follows :

(1) On the basis of the measurable voltage and current at the relay end, the value of angle γ, the fault resistance R_m and fault reactance X_m can be determined by eqn (3.15), and eqn. (3.16) respectively.

(2) The original operating characteristic boundary X can be adaptively changed to a new value X_B by using the information of angle γ, and through the following equation.

$$X_B = X + (R_m - R_Y) \cdot \tan\gamma \tag{3.17}$$

(3) The new boundary value X_B is now used for comparison with the original measured fault reactance X_m to determine if the fault is inside the protected region.

With today's powerful digital processors, it takes only a very short time to finish all the steps. The trigonometry term, $\tan\gamma$, may be a time consuming term in the fault calculation for the processor without the built–in trigonometry function. A simple angle–sum relation can be used for simplifying the operation.

$$\tan\gamma = \tan(\beta + \theta_Y) = \frac{\tan\beta + \tan\theta_Y}{1 - \tan\beta\tan\theta_Y}$$

where $\tan\theta_Y$ is calculated beforehand and $\tan\beta$ is given by the following equation.

$$\tan\beta = \frac{eh - fg}{eg + fh} \tag{3.18}$$

The above equation comes from the manipulation of the phasor I_0 (e, f) and the phasor of "$I_A + K I_0$" (g, h). In this way, $\tan\beta$ can be obtained directly from the sampled data.

3.4 Effect of taps

The preceding sections in this chapter have discussed the fundamental principles for dealing with the single line–to–ground fault and the problem associated with the effect of fault resistance and remote infeed has also been discussed. An adaptive protection method has been proposed in order to eliminate the error caused by this effect. The power system which the discussion is based on so far is a single transmission line system with the source and the load at each end, as the one shown in Figure 3.1. In many practical power systems, however, there are taps involved. In between the long distance of the transmission line which connects the generating plant and the major load center, there may exist several small communities. The most convenient way to supply electrical power to these users is using "taps" which are power transformers for stepping down the high voltage in the transmission line to a lower usable level. Figure 3.8 shows a typical power system with two taps connected as an example.

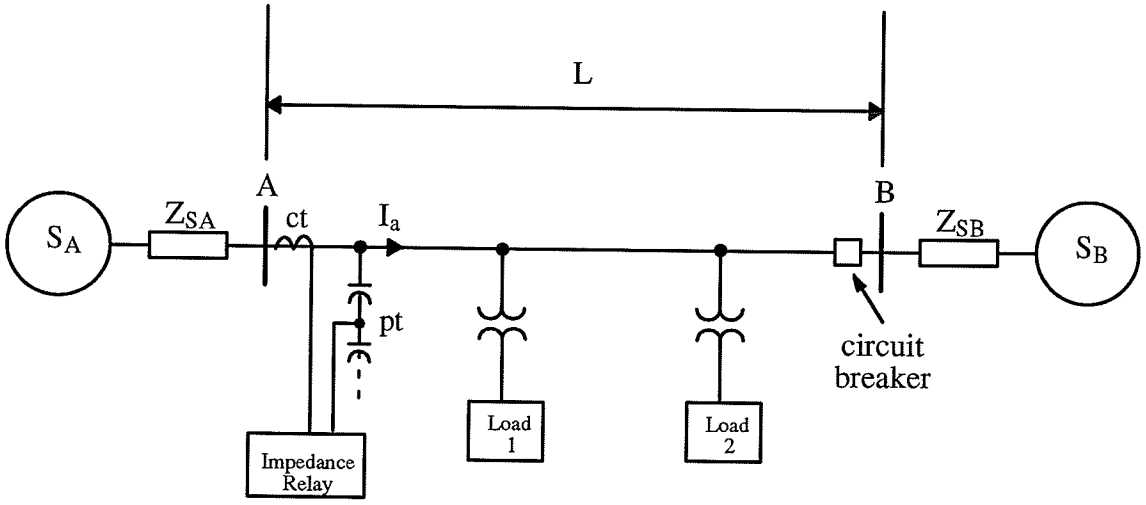

Figure 3.8 A typical power system with taps

Common three–phase transformers have several possible connections of the primary and secondary windings, such as having star–connected and earthed higher voltage windings and delta windings as the secondary windings, or a star–star connection with both neutrals grounded. Since the zero–sequence current will only flow if a return path exists, a delta–connected winding with no return path acts as an open circuit in the zero–sequence impedance network. Therefore, the zero–sequence equivalent circuits of three–phase transformers varies with the connections of the primary and secondary windings. For illustration, consider the connections shown in figure 3.9 where P and Q

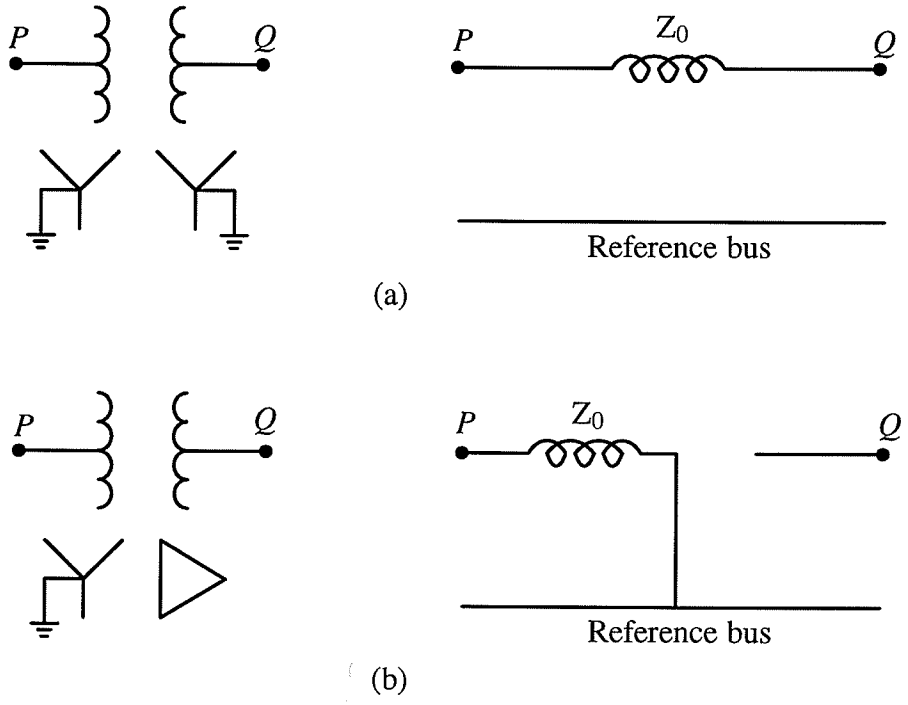

Figure 3.9 Zero–sequence equivalent circuits of three–phase transformer banks

are the corresponding points in the connection symbol diagram and the equivalent circuit. The star–star connected transformer shown in Figure 3.9a has both its neutrals grounded. A return path through the neutral therefore exists for the zero–sequence current to flow. The equivalent zero–sequence circuit is the one shown on the right. Figure 3.9b shows a

star–delta connection with the star connected side grounded. In this case the zero–sequence current can only flow through the star windings to the ground as the return path. The zero–sequence current in the delta windings which is induced by the current in the star windings, will flow in the loop of the windings without flowing out into the system. The resulting equivalent circuit is the one shown at the right where a path is connected with equivalent impedance of the transformer from point P to the ground (reference bus) on the star side. On the delta side, there is an open circuit between point Q and the reference bus.

The added taps on the transmission line cause problems when calculating fault impedance during single line–to–ground fault, since their existence can alter the sequence impedance network. When all the transformers have the high voltage star windings grounded, the impedances of the transformers appear in the zero–sequence impedance network as shown in Figure 3.10. Assuming a single line–to–ground fault at point F, the zero–sequence impedances for the taps are Z_{T1} and Z_{T2} respectively. The line impedance is divided into four fractions : m, n, o, and p. It is obvious that this impedance network is far more complex than the one shown in Figure 3.2c. Because there are only simple impedance loads behind the taps, the values of the positive and negative sequence impedances are relatively high in comparison to the line impedance. Therefore, the additional impedances do not appear in the positive and negative sequence networks. However, the zero–sequence network may differ considerably from the others due to the effect of different transformer windings and the reason has been described previously. The change in the zero–sequence impedance network affects the calculation of the K factor in eqn. (3.1) where K is equal to $\frac{Z_{0L} - Z_{1L}}{Z_{1L}}$ and Z_{0L} is the line zero–sequence impedance. Z_{0L} is now the equivalent zero–sequence impedance of the new zero–sequence impedance network seen at the relay location. Consequently, reevaluation of the K factor is required.

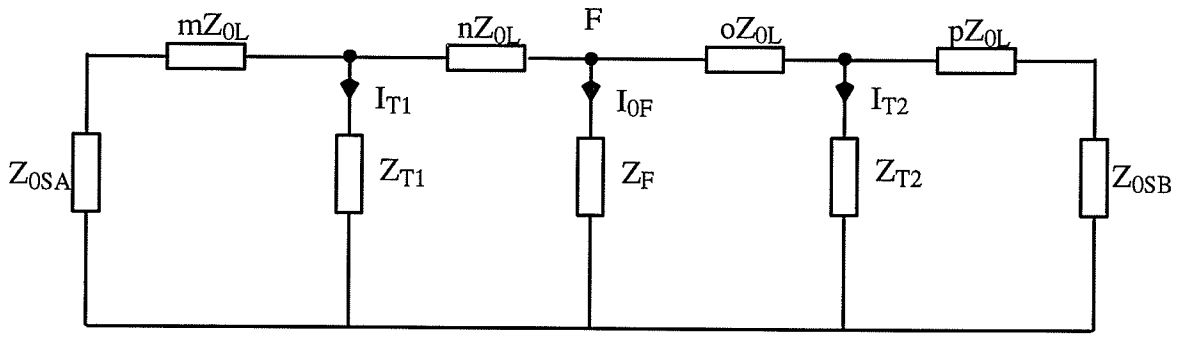

Figure 3.10 The altered zero–sequence impedance network

A possible problem may occur when the tap is off–line for some reason, The protective relay at one end may run into trouble if there is a single line–to–ground fault presented. The calculated fault impedance is wrong and causes maloperation of the relay, since the K factor is incorrect under this circumstance. The conventional protective relay without pilot communicating wires does not have the information as to whether or not the taps are on–line. A new idea to deal with such a problem is proposed here.

3.4.1 Adaptive method for dealing with the taps

The new technique tries to utilize the information of fault voltage and current measured at the relay end in order to adaptively change the K factor into a correct value. The ratio of $\frac{I_0}{I_1}$ is chosen to be the comparison factor since I_0 is changed dramatically between the system with or without the taps. For certain values of fault resistance, the I_0/I_1 ratio falls into a certain range of values. According to such a difference in the ratio, the presence of the taps may be recognized. The predetermined I_0/I_1 ratio can be obtained by running a system fault simulation. A set of pre–recorded I_0/I_1 ratios can be stored in the memories of the digital relay and is called up when under the fault situation. The values of K factor can be calculated by using the equation $\frac{Z_{0L} - Z_{1L}}{Z_{1L}}$. For a system

with taps, it should use the equivalent impedance value of the new zero–sequence impedance network seen at the relay location for Z_{0L}. Also, if the impedance loads behind the taps are small in comparison to the line impedance, it is necessary to calculate the equivalent impedance value of the changed positive–sequence impedance network for Z_{1L}. The pre–calculated values of K factor are then stored in the memory of the digital relay. A comparison is made between the calculated ratio from the measured quantities and the pre–recorded ratio. Then the K factor can be set accordingly.

The protection schemes mentioned in this chapter have been tested by using the Manitoba HVDC research centre's power system simulation program EMTDC. The results and discussion are included in the next chapter.

CHAPTER 4

EXPERIMENTAL RESULTS ON THE NEW ADAPTIVE ALGORITHMS

4.1 Power System Model

The relaying algorithms were tested on the transmission system model shown in Figure 4.1. This system represents the 230 kv line between Manitoba Hydro's Thompson and Ponton substations. A power source with equivalent source impedances is located at each end of the line. There are two taps connected between the main line and two locations—Pipe Lake and Dunlop. Sequence impedances of the sources, line and the taps

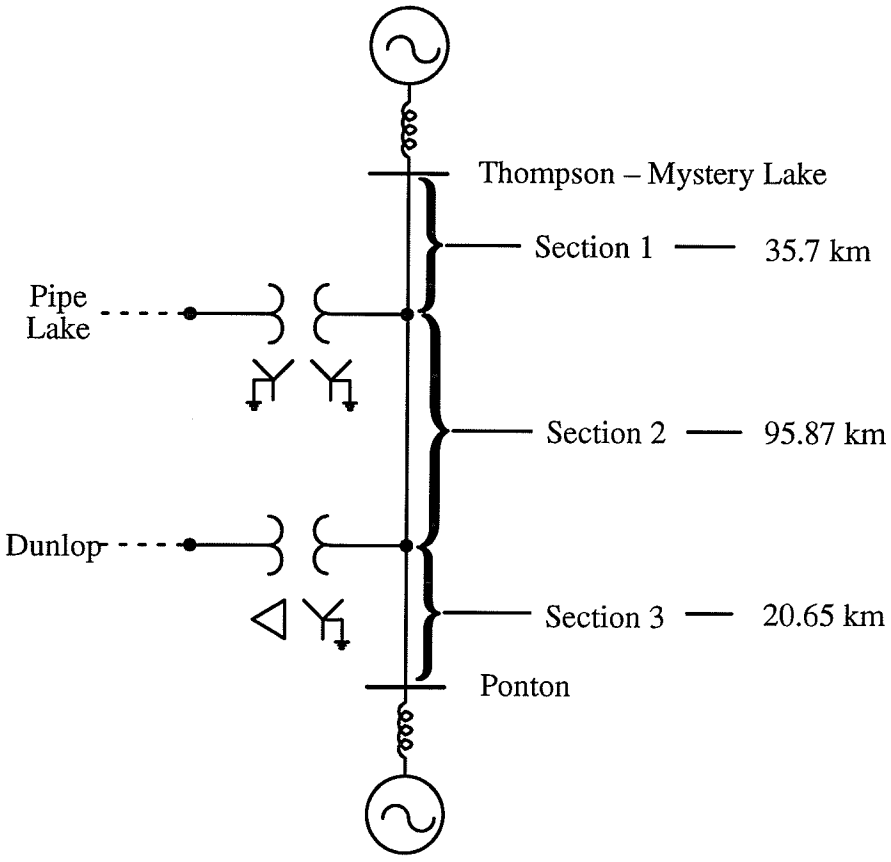

Figure 4.1 Transmission system model

are shown in the following tables. All the parameters are in per–unit form and the base of the model is 100 MVA.

	R_1	X_1	R_0	X_0
Thompson	0.0135	0.24920	0.00145	0.06360
Ponton	0.1109	0.13335	0.01448	0.11472

Table 4–1 Sequence impedances at Thompson and Ponton

Section	R_1	X_1	R_0	X_0
1	.0045	.0327	.0288	.1183
2	.0121	.0878	.0630	.2674
3	.0026	.0189	.0125	.0512

Table 4–2 Sequence impedances of the line

The tap connected between the main line and Pipe Lake is in the star–star connection with $Z_0 = j174\%$ to the 230 kV side. Meanwhile, the one between main line and Dunlop is in star–delta connection with $Z_0 = j57\%$ to the 230 kV side. The values of impedance loads behind the taps are, $Z_L = 0.3\angle 36°$, for a power factor equal to 0.8. The K factor for the system without taps based on the above system parameters is 2.19.

Power flow is simulated by using Manitoba HVDC centre's power system simulation program EMTDC. Several single line–to–ground faults with different magnitudes of fault resistance occurring near the remote boundary were simulated. The output data from the EMTDC program is filtered by a low–pass filter and the fundamental components of the waveforms are extracted by using the DFT algorithm. The relaying program which is responsible for applying the protection algorithm is written in the C computer language. All the simulations and tests were done on the Unix based Sun workstation.

4.2 Software Description

Figure 4.2 shows the fault processing flow chart which represents the actual program organization. The program is divided into several routines (function blocks). The advantage is that each function block can be modified individually for improving the performance of the relay. The program begins with a read and fault detection loop. The main task of this routine is to determine the state of the power system. In the normal nonfault condition, all voltages and currents are steady sinusoidal quantities. The method used in the program to detect a disturbance is a simple overcurrent detection. If the current is larger than a pre–set value, a disturbance is indicated and the program is entered into the fault state.

At the beginning of a fault state, a fault type identification routine will be executed. This routine determines the fault type so that the appropriate current and voltage pairs are selected for further fault calculation. The fault type classifying algorithm uses the concept of Clarke components and the actual development is included in Appendix III. One major reason to use a fault type classification routine is to provide the ability for the relay to handle all types of transmission line faults. The determination of R and X requires the major portion of the calculation time and the time to calculate R and X for all possible types represents a serious problem in maintaining high speed. With the fault type classification, only the appropriate current and voltage pairs are chosen for fault calculation, thereby avoiding unnecessary calculation. Although only the effect of single line–to–ground faults was concerned in the later tests, this routine provides an option for future relay function improvement.

Once the fault type is identified the program executes the fault calculation routine. The two proposed adaptive methods to correct the effects of fault resistance in single line–to–ground fault and taps were implemented in this routine. It is the task of this routine to adaptively change the operating characteristic or setting of the relay and

reports the calculated resistance and reactance. A counter is setup and whenever the values of Rm and Xm lie within the altered characteristic, the counter is increased. If the Rm and Xm values lie outside, the counter is decreased. For the security of the relay, the tripping count is set to 16 ($\frac{1}{2}$ cycle) of the tests. When the counter reaches the set value, the trip signal is issued.

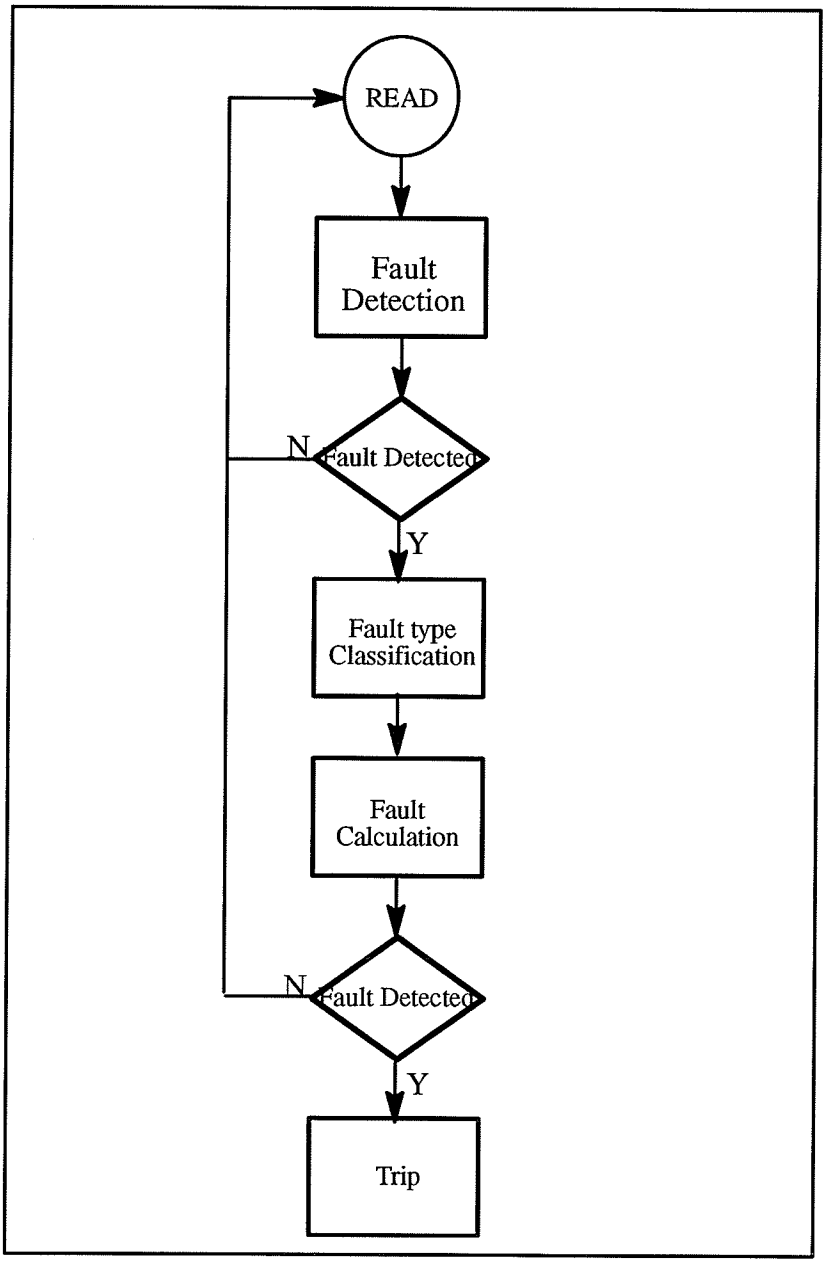

Figure 4.2 Fault Processing Flow Chart

4.3 Fault Calculation and General Test Results Overview

To illustrate the operation of the fault calculation routine, consider the simulation results shown in Figure 4.3 to Figure 4.8. Figure 4.3 and Figure 4.4 show the voltage and current waveforms generated by the EMTDC. A single line–to–ground at 78% of the line measured from Thompson with a fault resistance equal to 20 ohms was initiated at 0.1 sec. The system in Figure 4.4 is a special case in which a tap (Tap 2) with a star–delta connection is placed at 20% of the line beyond Thompson. The sketch of this system is the one on page 53A.

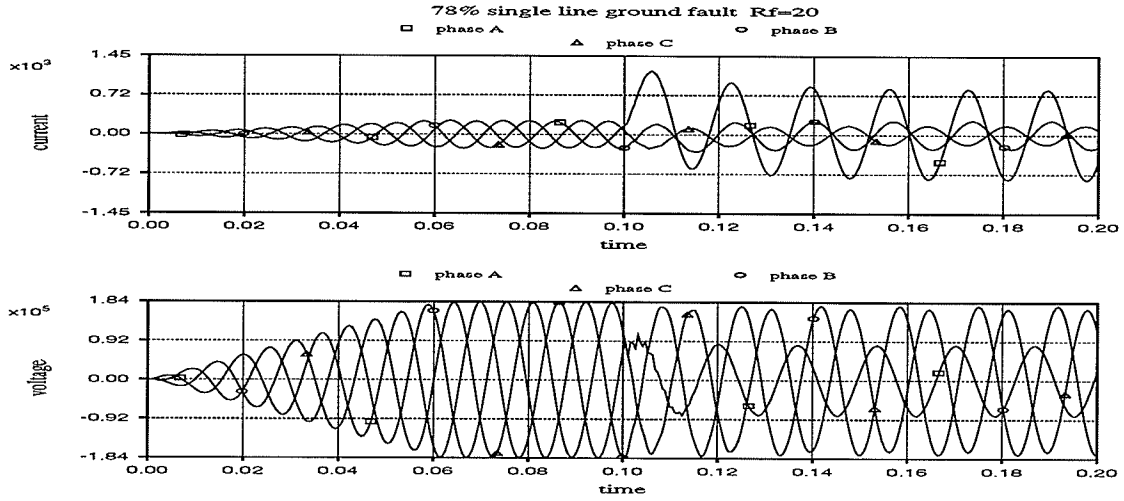

Figure 4.3 Waveforms for 78% SLG with $R_f = 20$ (without taps)

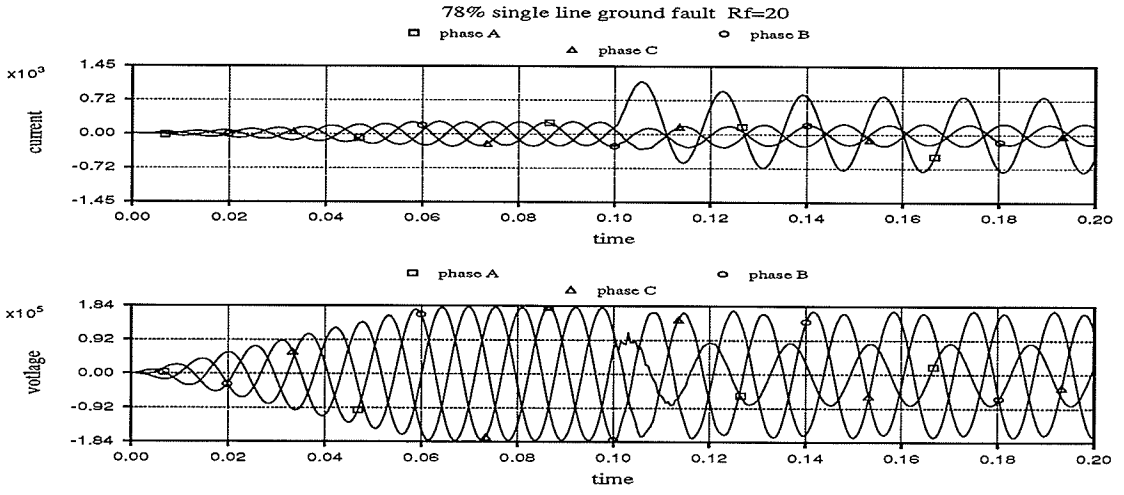

Figure 4.4 Waveforms for 78% SLG with $R_f = 20$ (with taps)

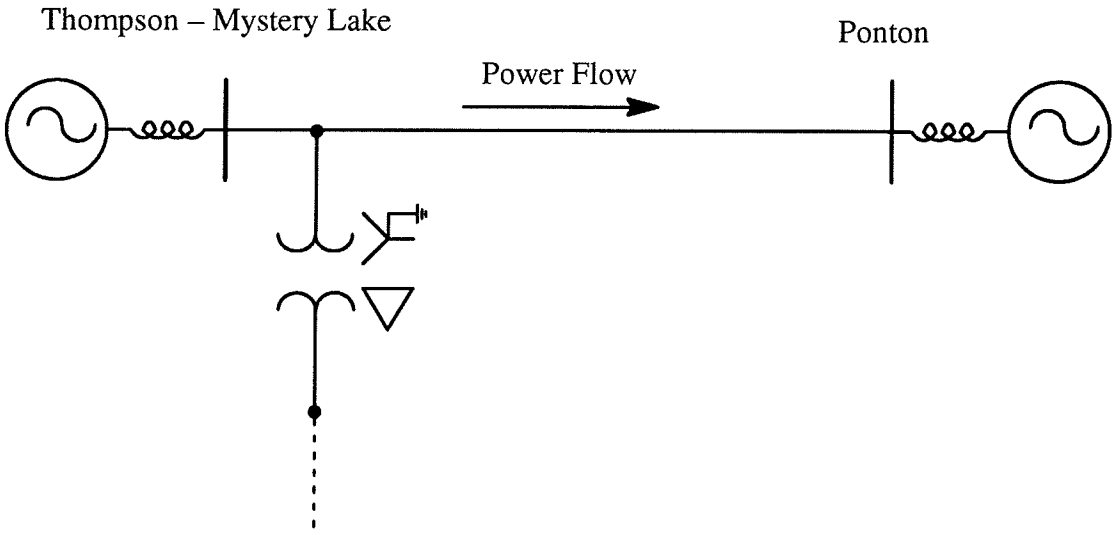
Thompson – Mystery Lake
Ponton
Power Flow

Figure 4.5 shows the measured values of tan β, R and X for the system without taps. Since a certain time period is required for the fault detection routine and type classification routine to detect and identify the fault, the evaluation of R and X can not be made until some time after the fault has been initiated. It is observed from the figures that this time period is about 3 msec. Once the fault calculation is started, the program will continue the fault processing for each subsequent data. When the measured resistance reaches the right hand resistance boundary, the program starts to compare the measured reactance with the upper reactance boundary. Before the comparison is made, the reactance boundary is rotated through an angle according to the information of beta.

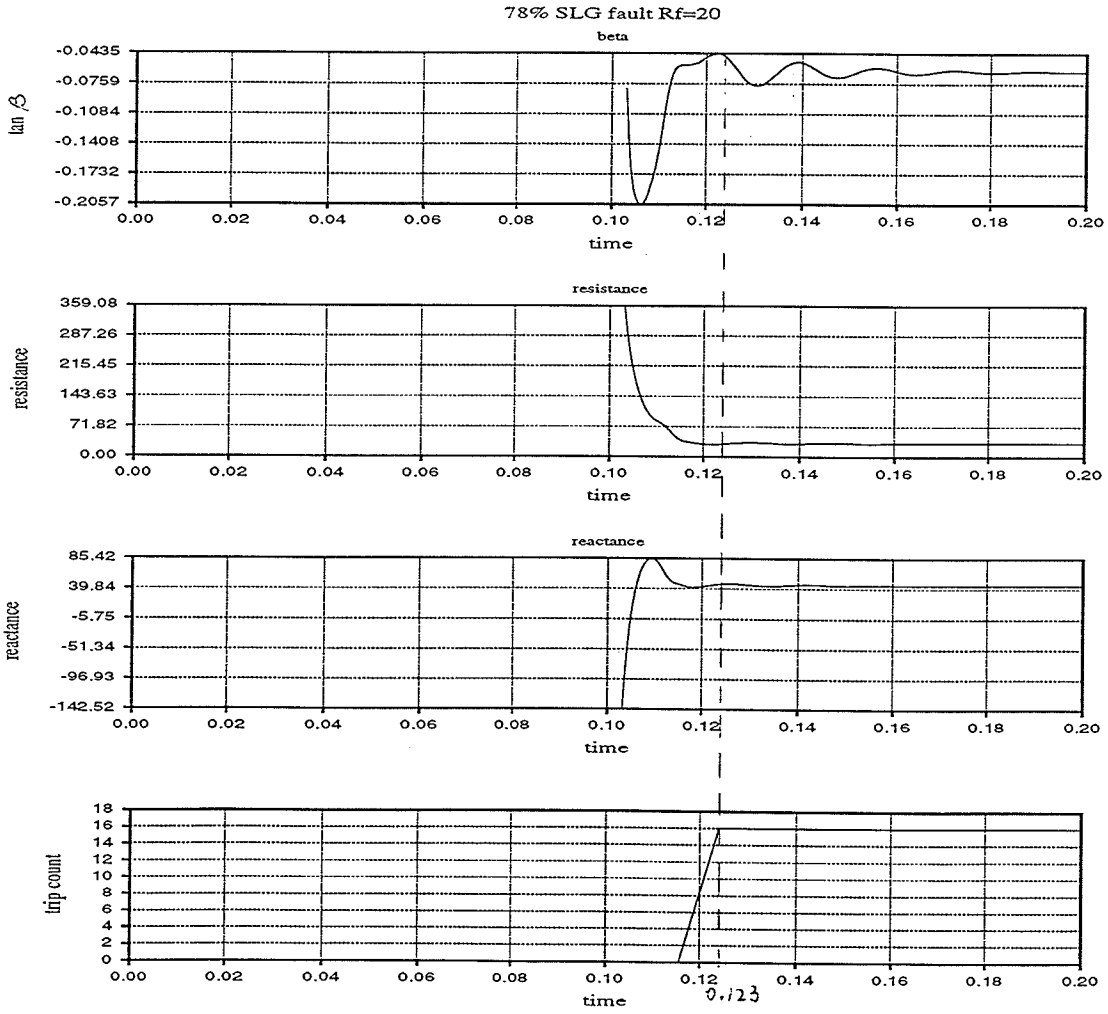

Figure 4.5 Measured resistance, reactance, beta and trip timing

When dealing with the taps, the ratio of I_0 / I_1 is calculated based on the current samples. Then according to this I_0 / I_1 ratio, the appropriate K factor is selected for fault impedance calculation. It is observed from the simulation results that the I_0 / I_1 ratios fall into certain ranges of values for certain values of fault resistance and fault locations. Also, the differences of these ratios between systems with or without taps were always greater than 20% (see Table 4–11, Table 4–12 and Table 4–13). For instance, when single line–to–ground faults occurred near 80% of the line beyond Ponton, the I_0 / I_1 ratios were always less than .55 when $R_f \leq 20$ and less than 0.65 when $20 \leq R_f \leq 50$ for a system with taps. Also, the ratios are always less than .75 when $R_f \leq 20$ and less than 0.89 when $20 \leq R_f \leq 50$ for a system with taps and faults occurring around 40% to 60% of the line beyond Ponton (see Table 4–13). Therefore, several regions for I_0 / I_1 ratio comparison were setup in the tests (for faults located < 15% of the line beyond Ponton, 15% to 40%, 40% to 60%, 60% to 75% and 75% to 85%). In the case when a fault occurs near the region's boundary the calculated fault impedance value may fall into the next region. The comparison factors were setup in such a way that no matter which region the fault falls into it would produce a valid comparison under such a condition. In order to determine which region the fault impedance lies within, the first fault impedance value is calculated by using the K factor for a system with taps. This fault impedance value may not be correct, but it does give an indication of the location of the fault. Once the region is known then the comparison for I_0 / I_1 ratio can be made and the K factor set accordingly. Although the I_0 / I_1 ratios may vary for a system with a different configuration, the idea for setting up a comparison region is the same. Figure 4.6 shows the I_0 / I_1 ratio with and without taps for a system with waveforms shown in Figure 4.3 and Figure 4.4. Also, the timing for the trip counter is shown in the figures. The trip times for the relay are marked in the figures.

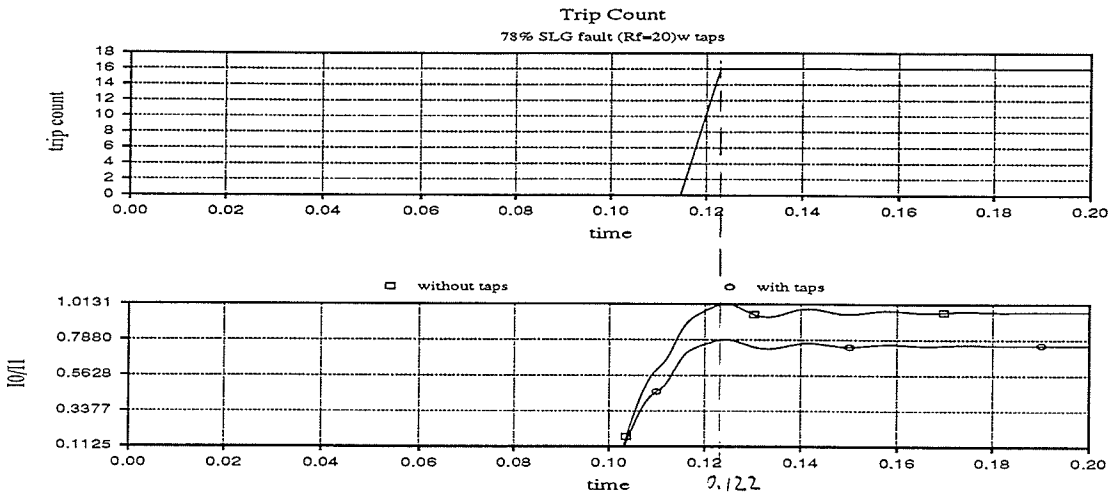

Figure 4.6 I_0 / I_1 ratio and trip timing

The relay operating characteristics used during testing are shown in Figure 4.7. The upper reactance boundary was set at 80% of the protected line. The left hand limit was set arbitrarily at R = 0 ohms. The right hand resistance boundary was set at 100 ohms. The reason for such a high resistance boundary setting is to investigate the effect of high fault resistance. In practical application, the setting of this resistance boundary should be under the constraints of system load conditions. Several tests have been done for fault conditions with a lower resistance boundary setting (50 ohms). There is no major difference of the relay operation between these two different settings. However, the relay with lower resistance boundary would not trip on faults with higher fault resistance than the boundary setting. The impedance trajectories for single line–to–ground fault at (a) 78% of the line with fault resistance equal to 20 ohms and (b) 82% of the line with fault resistance equal to 30 ohms are shown in Figure 4.7. In the figure, (a1) and (b1) show the impedance trajectories with the fixed boundary. It is shown in (b1) that the out of zone fault dropped into the operating zone and caused maloperation. Figure (a2) and (b2) show the upper reactance boundary started to rotate as the impedance trajectories have reached the right resistance boundaries. The final

boundary characteristics are shown in (a3) and (b3). It is shown in the figures that the reactance boundaries have altered correctly and no maloperation is recorded.

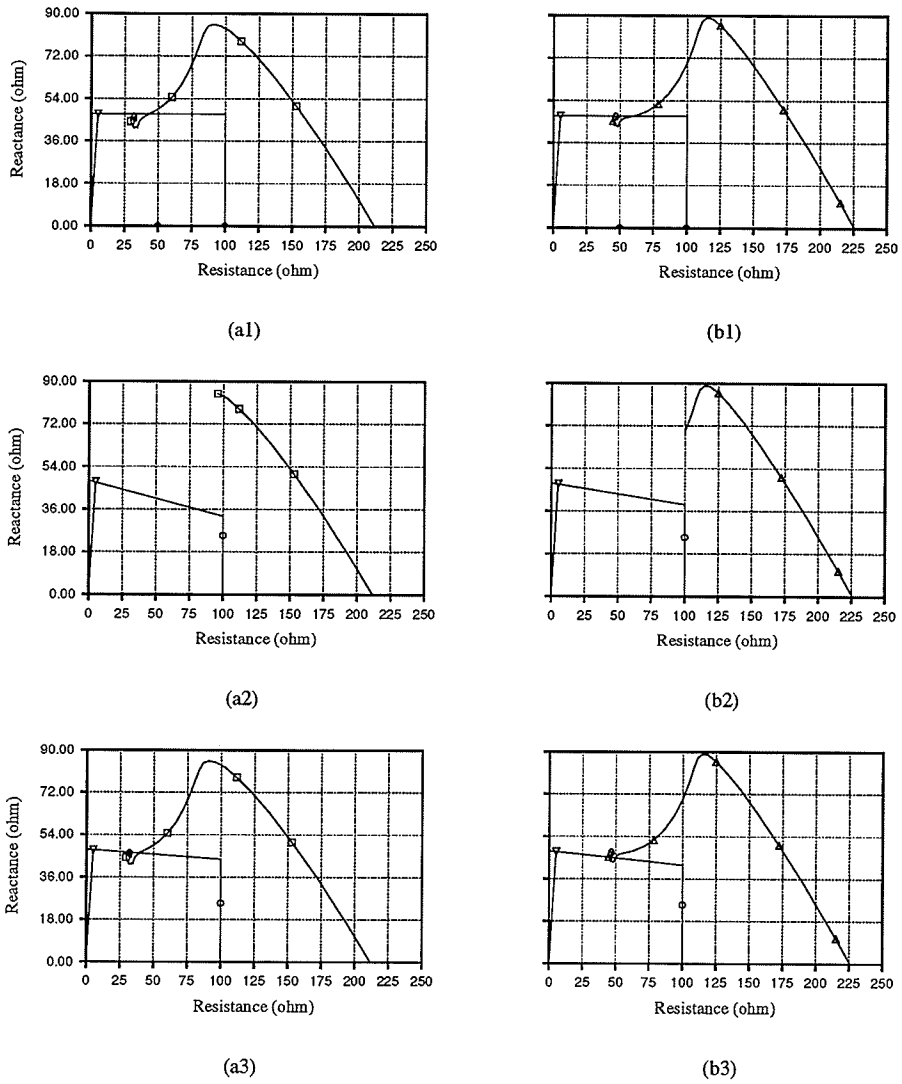

Figure 4.7 Impedance trajectories

When subjected to reverse faults, the current waveform reversal causes a high impedance trajectory in the fourth and third quadrants before the output settles to its fault value. The relay characteristic is thus in no danger of being tripped. Such a fault is shown in Figure 4.8. The figure on the left is the original impedance trajectory and the one on the right hand side is the enlarged impedance trajectory near the boundary. (The reverse fault was created right behind the location of the relay, therefore, its final fault value is very close to the origin of the boundary of the relay).

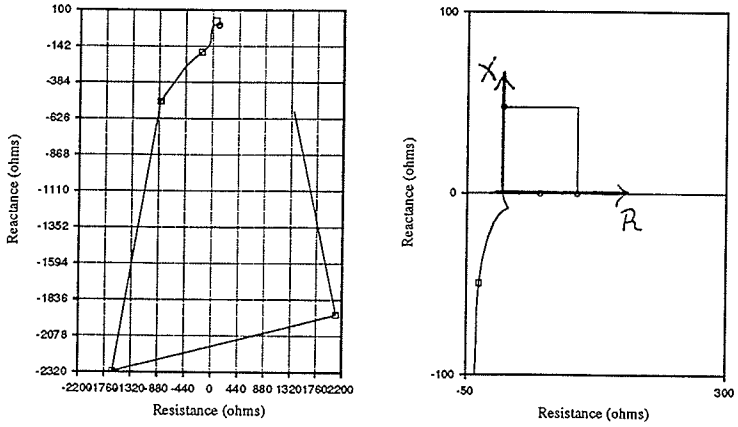

Figure 4.8 Impedance trajectory for reverse fault

In the following sections, a series of simulation results are presented for faults under different fault resistance and tap conditions.

4.4 Test of effect of ground fault resistance and remote infeed

In the first set of tests, taps were removed from the system for observing the effect of ground fault resistance only. A zone 1 protection was setup and the boundary was set at 80% of the line measured from the relay location. The characteristic for the relay tripping was programmed as a generalized quadrilateral, such as the ones shown in chapter 3. In the simulation, the direction of power flow is always from Thompson to Ponton (230kv, 70MW).

a) At Thompson

The setup is illustrated in Figure 4.9. In the first test, the relay was sitting at the Thompson end and point Y was the 80% boundary. F_1 and F_2 were two points located at the 78% and 82% of the line respectively.

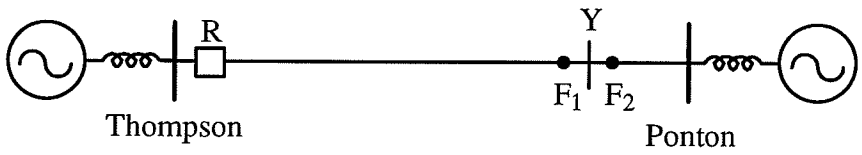

Figure 4.9 Transmission system model

Single line–to–ground faults were applied at points F_1 and F_2 with different fault resistances (0 – 50 ohms) between the faulted line and the ground. Some of the results are recorded in the following tables where R_m and X_m are the measured resistance and reactance at the relay end.

R_f	R_m	X_m
0	5.02	46.12
10	18.79	45.88
20	32.33	45.35
30	45.67	44.61
40	58.23	43.72
50	70.54	42.69

Table 4–3 78% Single line–to–ground fault (without taps) At Thompson

R_f	R_m	X_m
0	5.31	48.33
10	19.55	48.08
20	33.53	47.51
30	47.08	46.73
40	60.23	45.79
50	72.91	44.71

Table 4–4 82% Single line–to–ground fault (without taps) At Thompson

For a better illustration, please refer to the following figure where the solid horizontal line represents the fixed 80% boundary line. It is obvious that the out of zone fault would eventually drop into the protected region with the increasing of fault resistance and cause a mis–operation of the relay.

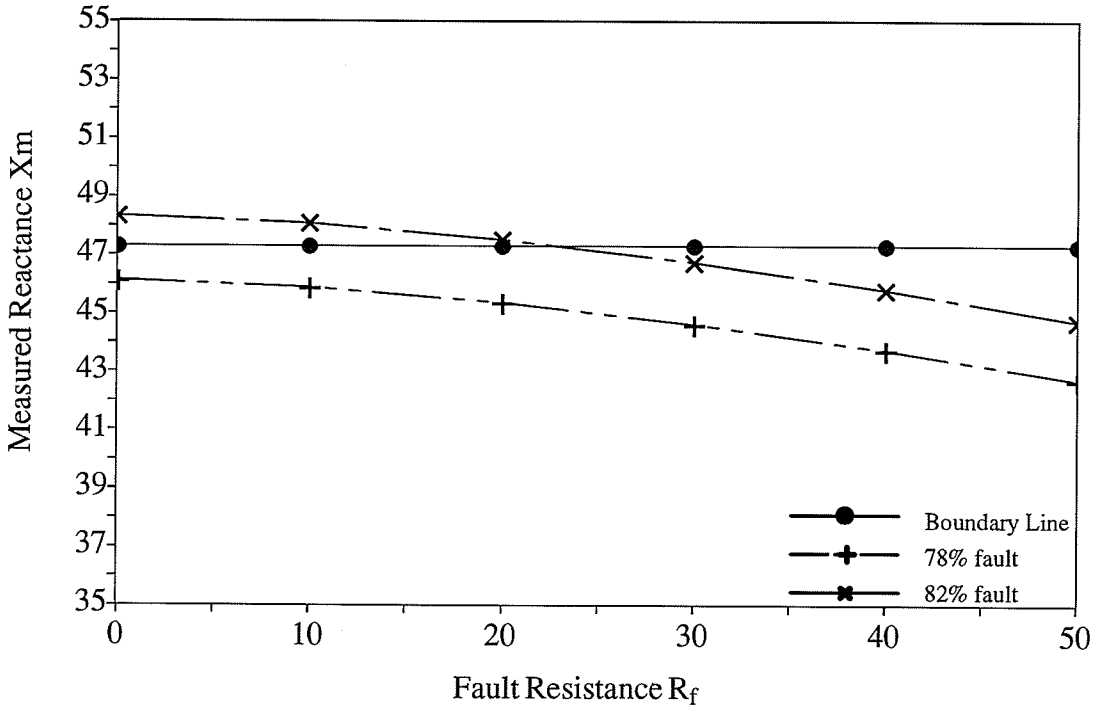

Figure 4.10 Effect of ground fault resistance at Thompson

With the adaptive feature, Figure 4.11 and 4.12 show that the reactance boundary has varied adaptively in the tests. Figure 4.11 shows that the measured reactance is always less than the altered reactance boundary when single line–to–ground faults occur within the protected zone 1. Meanwhile, Figure 4.12 shows the measured reactance is always greater than the altered reactance boundary when single line–to–ground faults occur outside the protected zone 1. The results are also recorded in the following tables. Table 4–5 also shows the operating times for this adaptive relay.

R_f	X_m	X_b	trip time (msec)
0	46.12	47.30	23.96
10	45.88	46.81	23.44
20	45.35	46.13	22.34
30	44.61	45.30	22.92
40	43.72	44.30	22.92
50	42.69	43.17	21.36

Table 4–5 78% Single line–to–ground fault At Thompson

R_f	X_m	X_b
0	48.33	47.30
10	48.08	46.80
20	47.51	46.12
30	46.73	45.26
40	45.79	44.23
50	44.71	43.06

Table 4–6 82% Single line–to–ground fault At Thompson

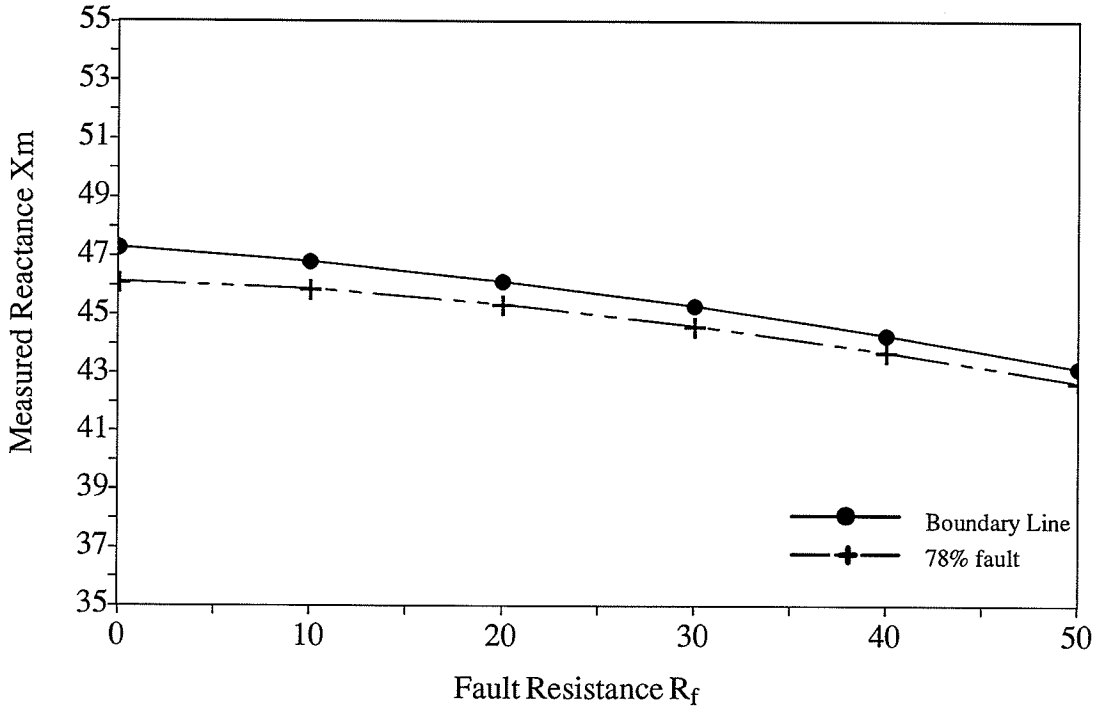

Figure 4.11 Altered boundary with ground–fault (78%)

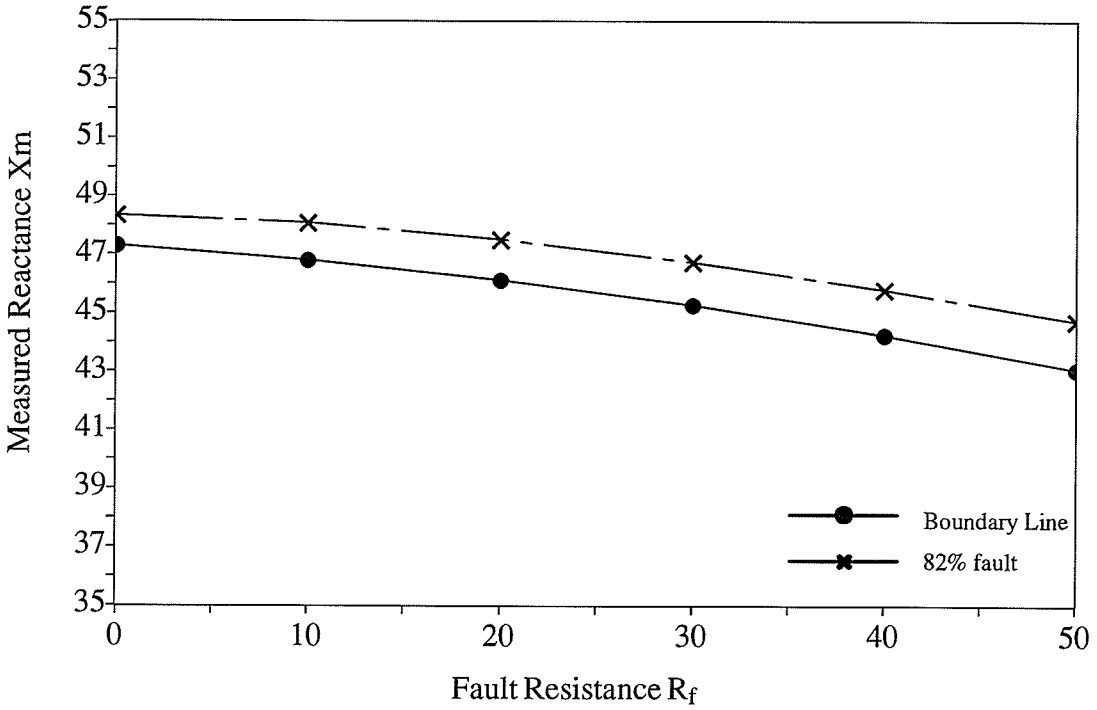

Figure 4.12 Altered boundary with ground–fault (82%)

b) At Ponton

The second test was setup just as for the first one, but this time the relay was sitting at the Ponton end and the boundary was set at the other end as shown in Figure 4.13. The direction of power flow is also from Thompson to Ponton with the same magnitude as before.

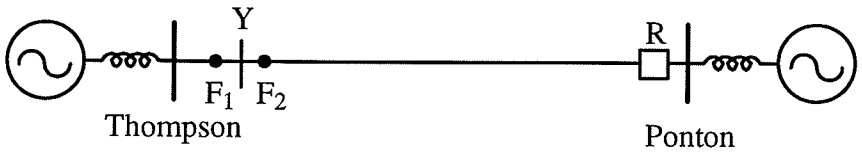

Figure 4.13 Transmission system model

Again, single line–to–ground faults were applied at points F_1 and F_2 with different fault resistances. The test results are recorded in the following tables.

R_f	R_m	X_m
0	6.7	51.78
10	22.00	52.44
20	37.97	53.00
30	54.67	53.59
40	71.85	54.22
50	89.76	54.89

Table 4–7 78% Single line–to–ground fault (without taps) At Ponton

R_f	R_m	X_m
0	7.12	54.31
10	22.99	54.97
20	39.59	55.52
30	56.86	56.10
40	74.87	56.71
50	93.55	57.36

Table 4–8 82% Single line–to–ground fault (without taps) At Ponton

The data from the above tables are plotted in Figure 4.14. Since the power was flowing into the relay location, it pushed the out of zone fault further away from the fixed boundary. There is no danger for the relay to misoperate in this case. However, for the in–zone fault, the measured impedance X_m dropped out of the relay operating region to cause failure to trip when fault resistance was greater than 20 ohm.

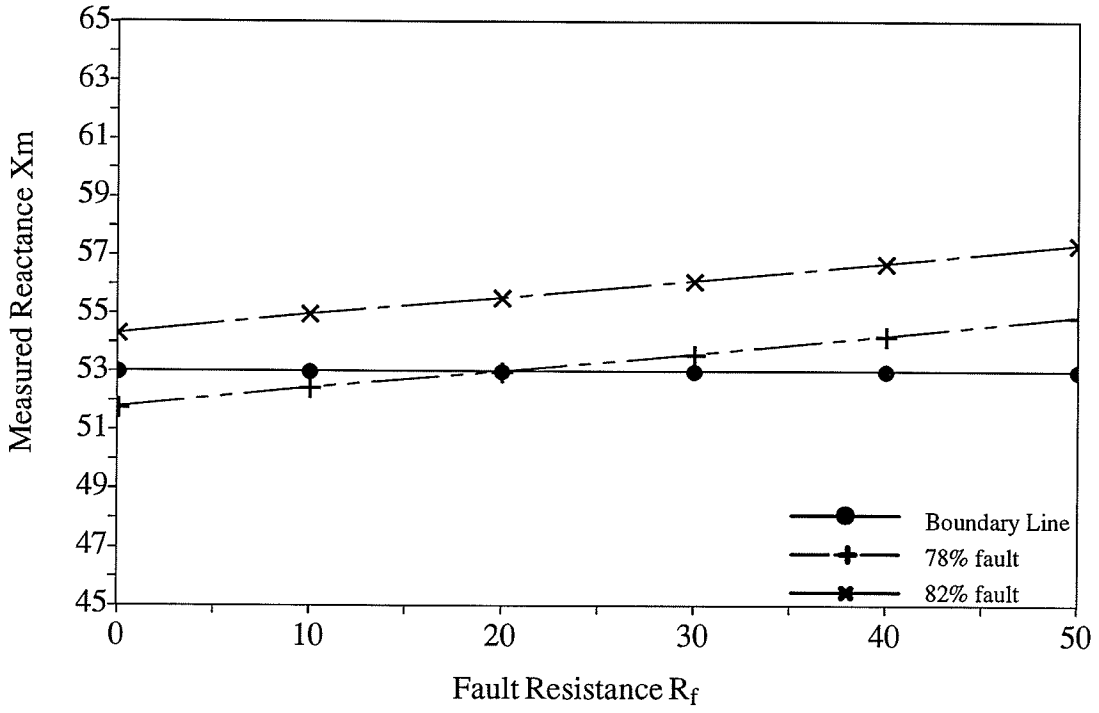

Figure 4.14 Effect of ground fault resistance At Ponton

With the adaptive feature, Figure 4.15 and 4.16 show that the reactance boundary again has varied adaptively in the tests. Figure 4.15 shows that the measured reactance is always less than the altered reactance boundary when single line–to–ground faults occur within the protected zone 1. Meanwhile, in Figure 4.16 the measured reactance is always greater than the altered reactance boundary when single line–to–ground faults occur outside the protected zone 1. The results are once again recorded in the following tables with the operating times.

R_f	X_m	X_b	trip time (msec)
0	51.78	52.99	23.96
10	52.44	53.34	23.44
20	53.00	53.73	22.92
30	53.59	54.17	22.92
40	54.22	54.67	22.40
50	54.89	55.22	24.48

Table 4–9 78% Single line–to–ground fault At Ponton

R_f	X_m	X_b
0	54.31	53.01
10	54.97	53.46
20	55.52	53.95
30	56.10	54.51
40	56.71	55.13
50	57.36	55.81

Table 4–10 82% Single line–to–ground fault At Ponton

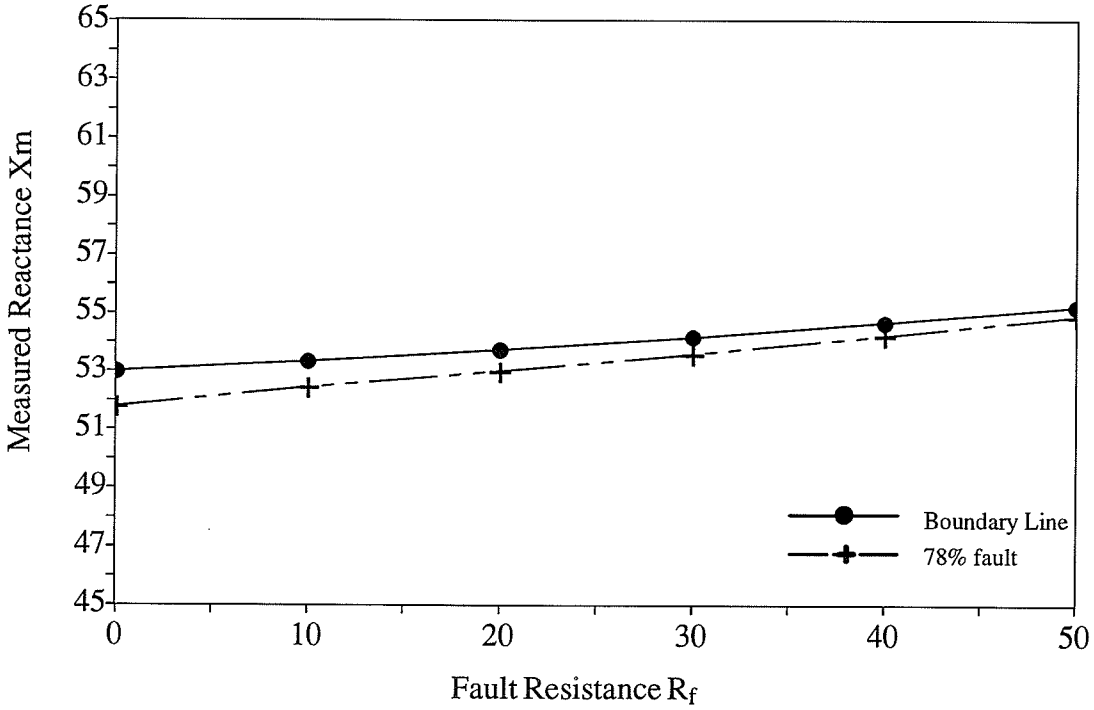

Figure 4.15 Altered boundary with ground–fault (78%)

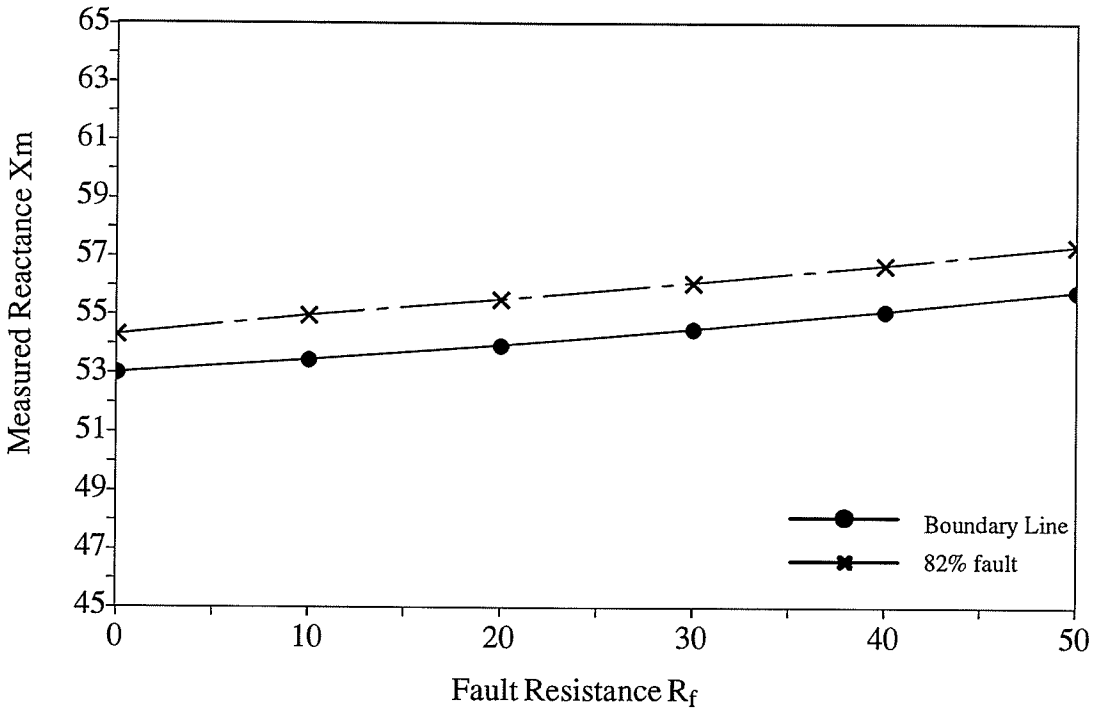

Figure 4.16 Altered boundary with ground–fault (82%)

From the above tests, it is shown that the digital relay has operated correctly and was not affected by a fault resistance up to 50 ohms when the faults occur in the neighborhood (± 2%) of the zone 1 boundary. Moreover, it is observed that the reactance boundary has automatically rotated in the correct direction according to the direction of the prefault load flow and did not require pre–adjustment.

Also, it is observed in many tests that the time from a fault initiation until issue of the tripping signal of the relay is always less than 2 cycles for faults within zone 1. The operating time may be reduced by using a shorter trip count (trip count was set at 16).

Moreover, the security of the relay with an adaptive protection scheme is not degraded for faults which do not occur near the remote boundary. It is illustrated by Figure 4.17, where a single line–to–ground fault was applied at 60% of the line measured from Thompson with a different fault resistance. The operating time for the relay is also marked on the figure. From the figure, it is obvious that the measured

reactance is always well within the protected region and maloperation did not occur in the tests. Therefore, the digital relay equipped with this adaptive feature is suitable for a general distance protection application.

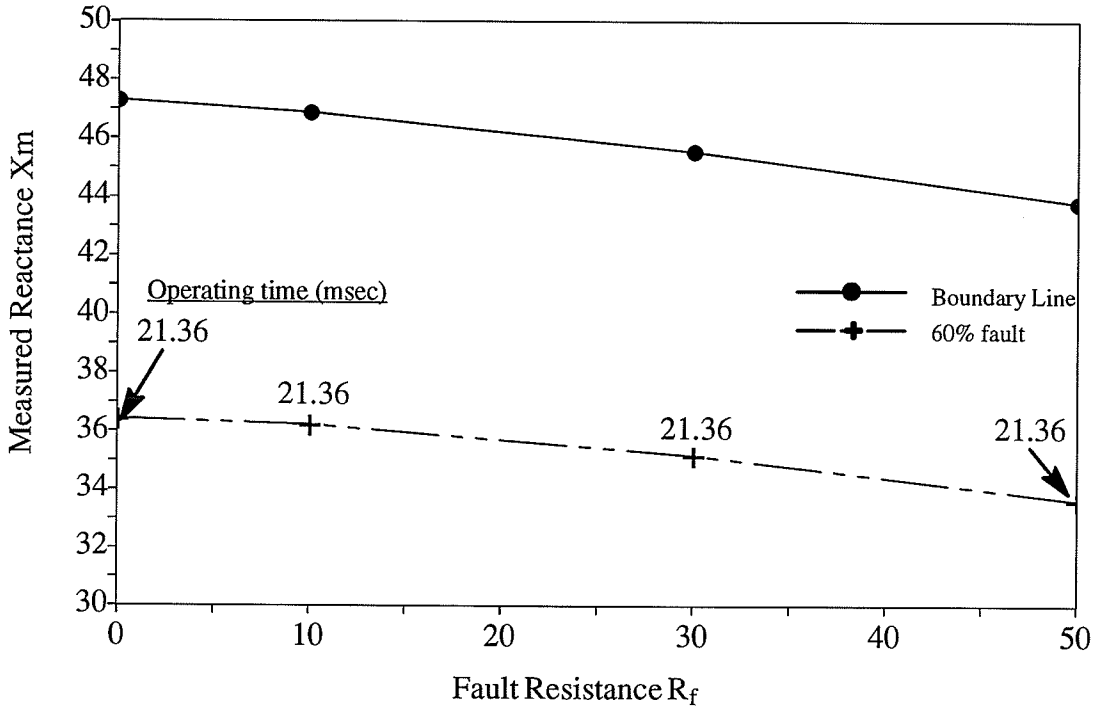

Figure 4.17 60% Single line–to–ground fault (Thompson)

4.5 Test of the effect of taps

The effects of taps on the power system were studied by using the system model shown in Figure 4.1. Again, the power flow is from Thompson to Ponton and the tests were done on each end of the line.

a) At Thompson

Single line–to–ground faults were applied at 78% and 82% of the line individually. Figure 4.18 and Figure 4.19 show that the effects of taps on the system are insignificant. This is because tap 1 consists of a star–star connection with relatively high zero–sequence impedance and acts as an open circuit. Tap 2 is located beyond the faults and the I_0 signal received by the relay is dominated by the fault branch. This condition was tested further by applying the ground fault at 60% of the line. Figure 4.20 shows that the effect is again insignificant. Therefore, the impact of the taps on the system is minimal in this case. It was decided not to perform the adaptive protection scheme here.

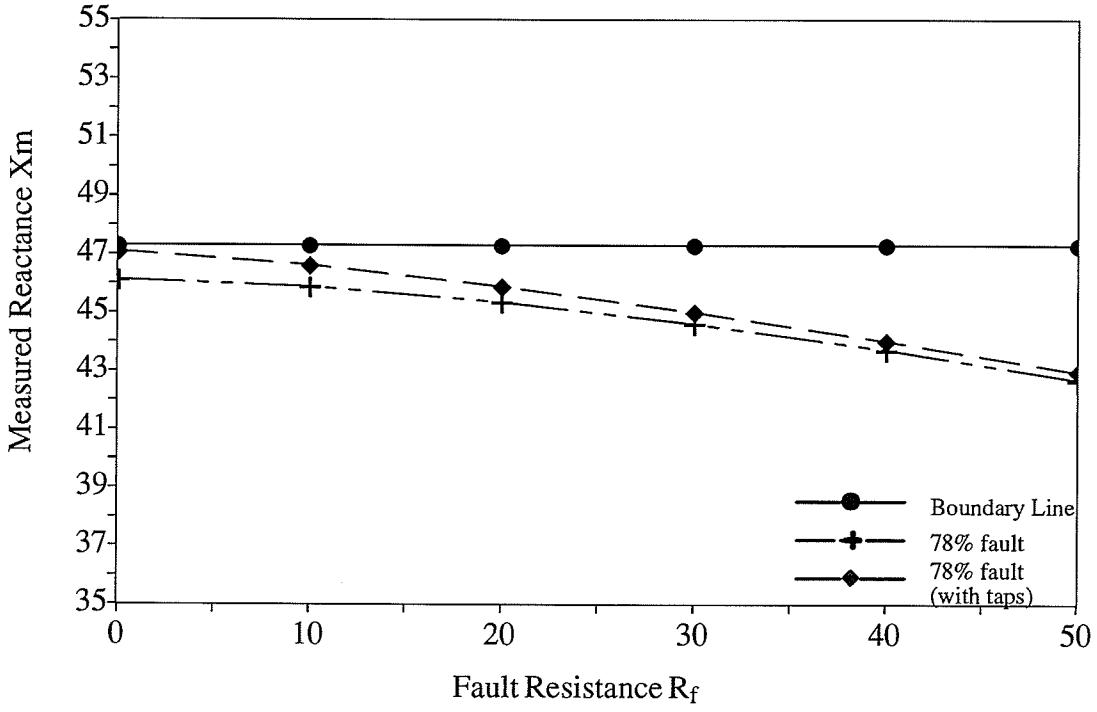

Figure 4.18 78% Single line–to–ground faults (with taps) At Thompson

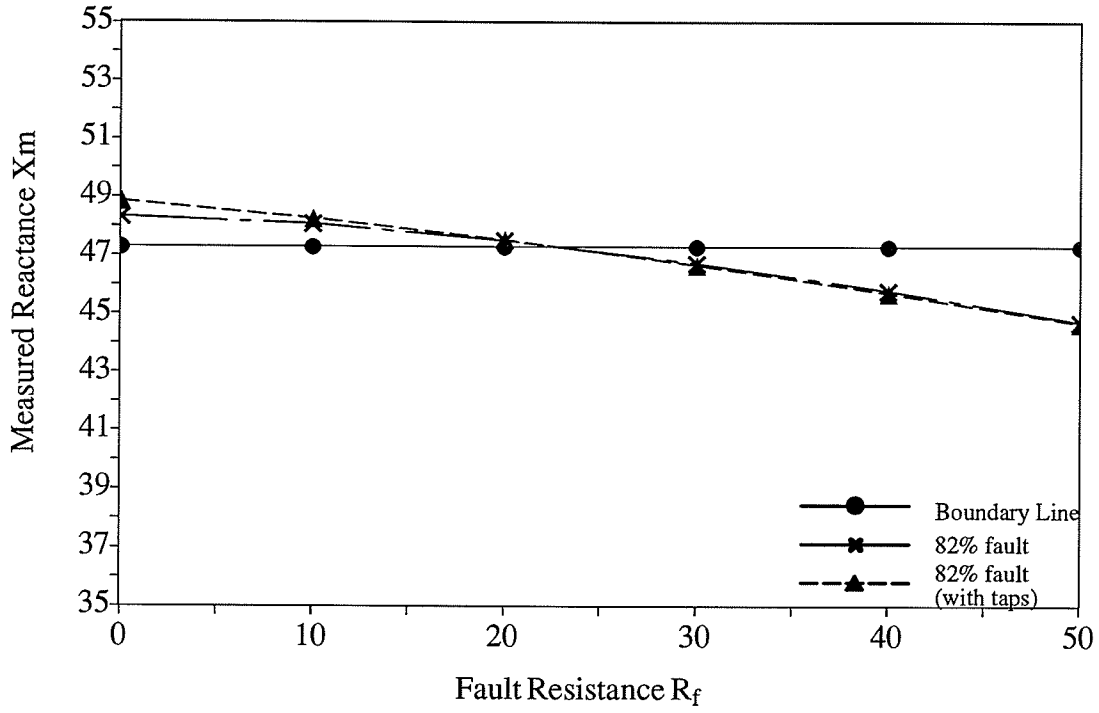

Figure 4.19 82% Single line–to–ground faults (with taps) At Thompson

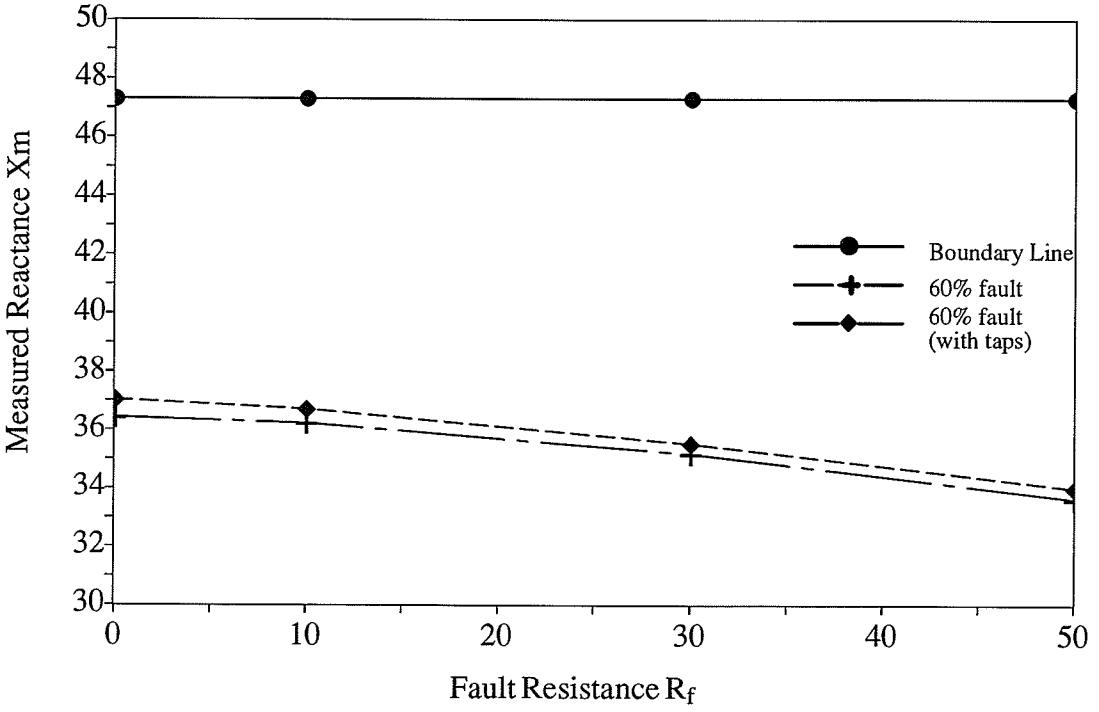

Figure 4.20 60% Single line–to–ground faults (Thompson)

b) At Ponton

Figure 4.21 and Figure 4.22 show the effects of taps under single line–to–ground fault with different fault resistance condition. For faults measured at the Ponton end, tap 2 is located in front of the faults. It is shown that the measured reactance is very different from the one without taps.

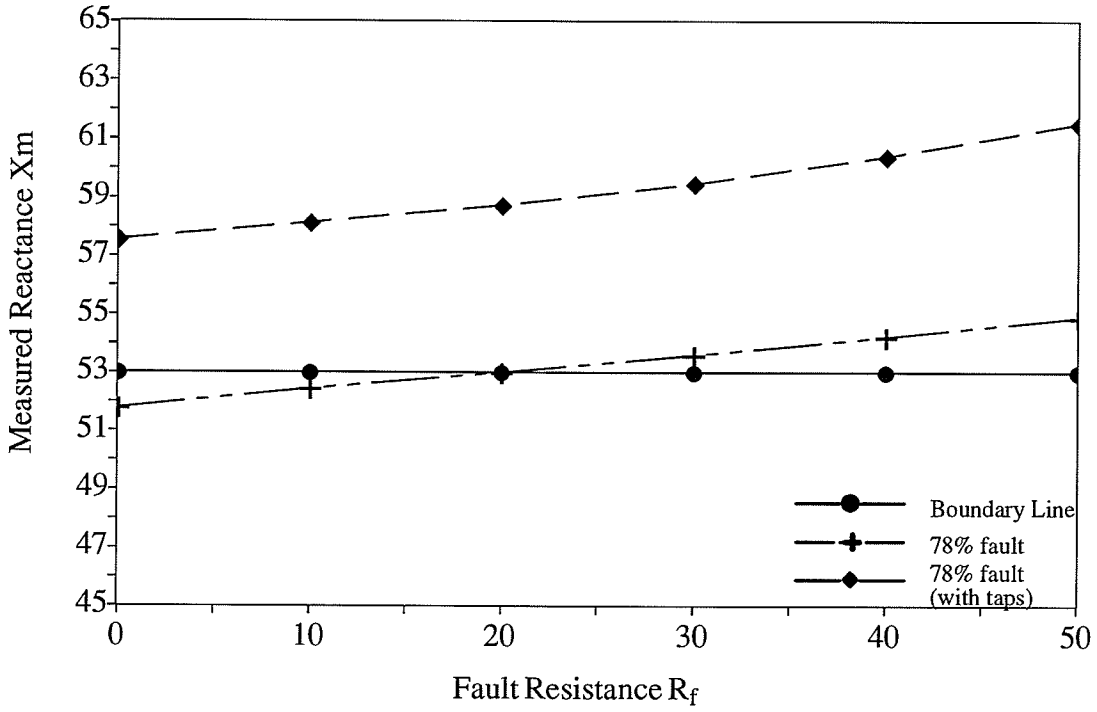

Figure 4.21 78% Single line–to–ground faults (with taps) At Ponton

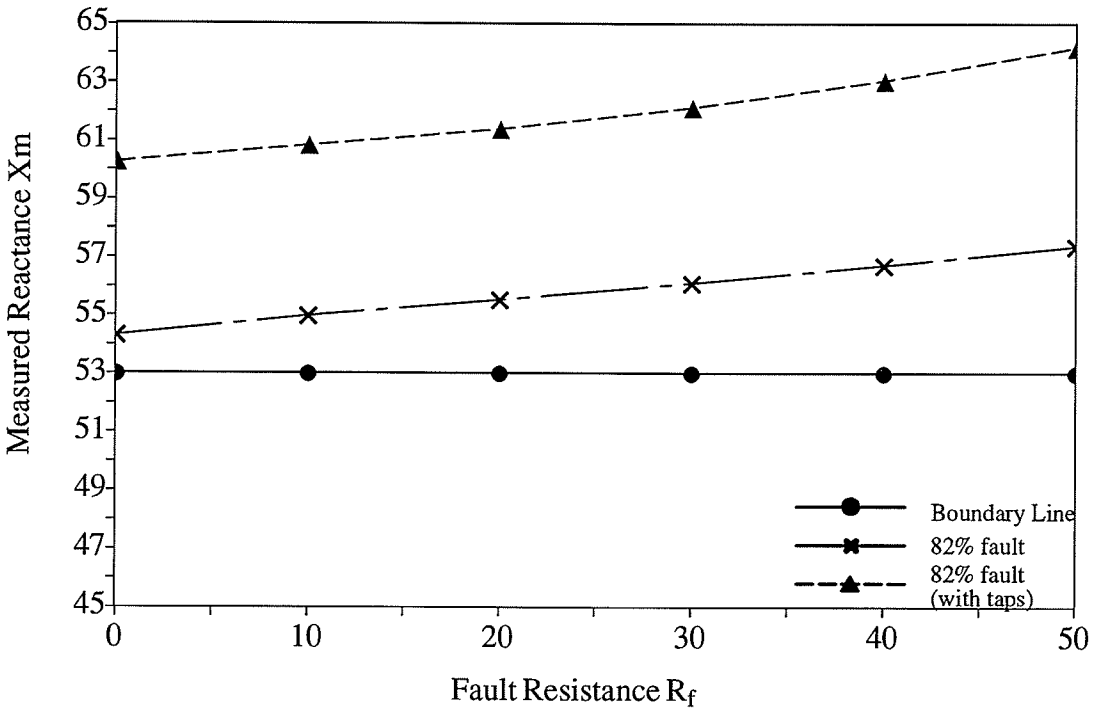

Figure 4.22 82% Single line–to–ground faults (with taps) At Ponton

The adaptive scheme was applied and the digital relay was programmed to respond to the difference in the I_0 / I_1 ratio and to use the predetermined K factor to calculate the reactance and resistance. The predetermined K factor for a system with taps in this case is 2.41 (the K factor for a system without taps is 2.19). However, based on the early test results, refinements were made to the setting to increase the accuracy of the fault impedance calculation. The adjusted value for K factor used in the tests is 2.6 for a system with taps. The difference in the I_0 / I_1 ratio is recorded in Table 4–11 and Table 4–12. The results are shown in Figure 4.23 and Figure 4.24. From the figures, it is shown that the measured reactances are very close to the ones for a system without taps.

R_f / I_0/I_1	0	10	20	30	40	50
without taps	0.62	0.66	0.70	0.76	0.82	0.89
with taps	0.47	0.49	0.52	0.55	0.58	0.61
difference in %	24.19	25.75	25.71	27.63	29.27	31.46

Table 4–11 78% Single line–to–ground fault (with taps) At Ponton

R_f / I_0/I_1	0	10	20	30	40	50
without taps	0.59	0.63	0.68	0.73	0.79	0.86
with taps	0.45	0.48	0.50	0.53	0.56	0.59
difference in %	23.72	23.81	26.47	27.40	29.11	31.40

Table 4–12 82% Single line–to–ground fault (with taps) At Ponton

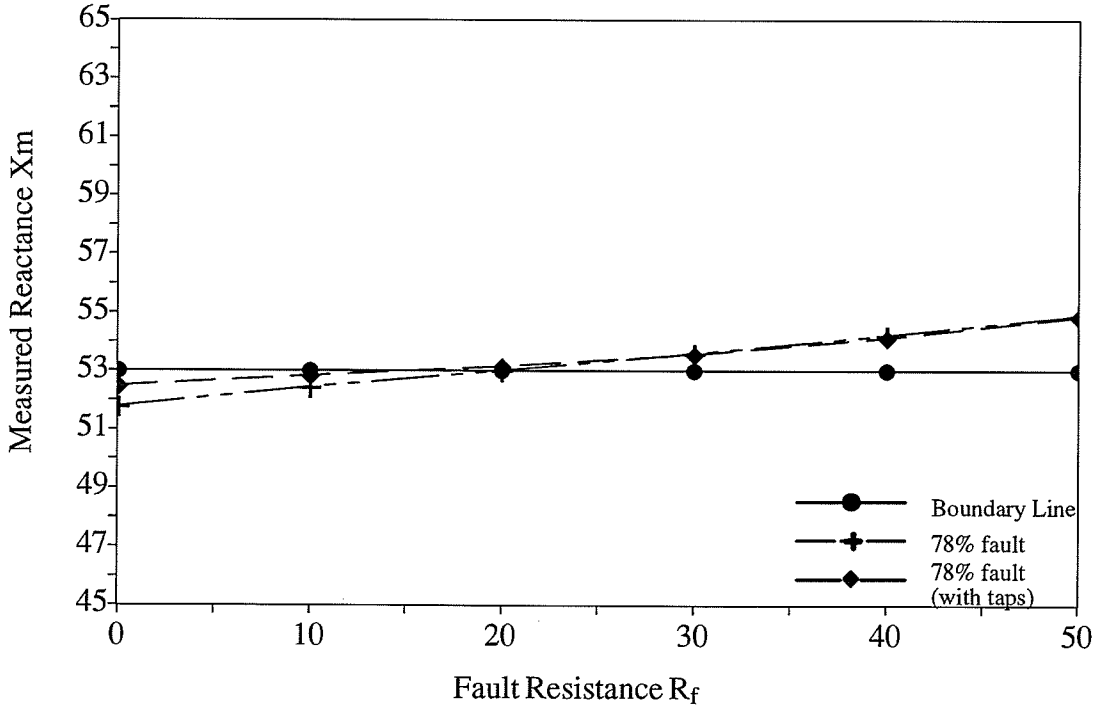

Figure 4.23 78% Single line–to–ground fault (with taps)

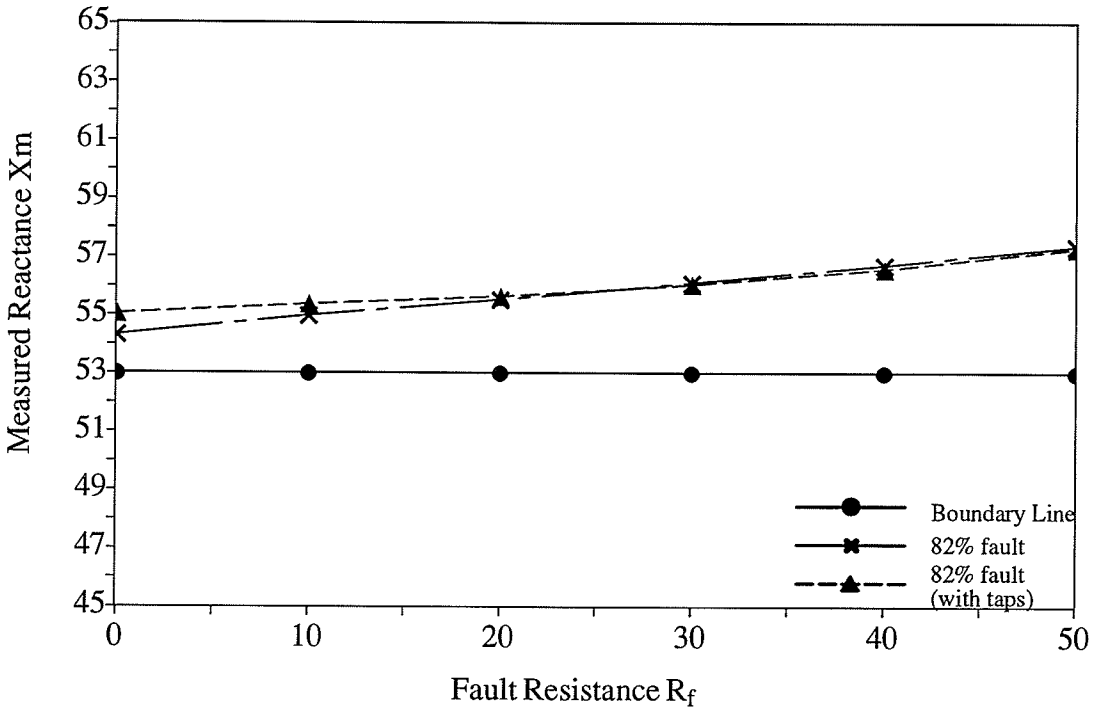

Figure 4.24 82% Single line–to–ground fault (with taps)

For further examination, a single line–to–ground fault was applied at 40% of the line with and without the taps. In the test, the relay was able to recognize the difference and was not under the influence of a fault resistance up to 50 ohms. Figure 4.25 shows the measured reactance without the adaptive protection scheme. Figure 4.26 shows the reactance reported by the relay with the adaptive protection scheme. The I_0 / I_1 ratio are recorded in the following table.

R_f / I_0 / I_1	0	10	30	50
without taps	0.86	0.91	1.04	1.19
with taps	0.67	0.70	0.76	0.84
difference in %	22.09	23.07	26.92	29.41

Table 4–13 40% Single line–to–ground fault (with taps) At Ponton

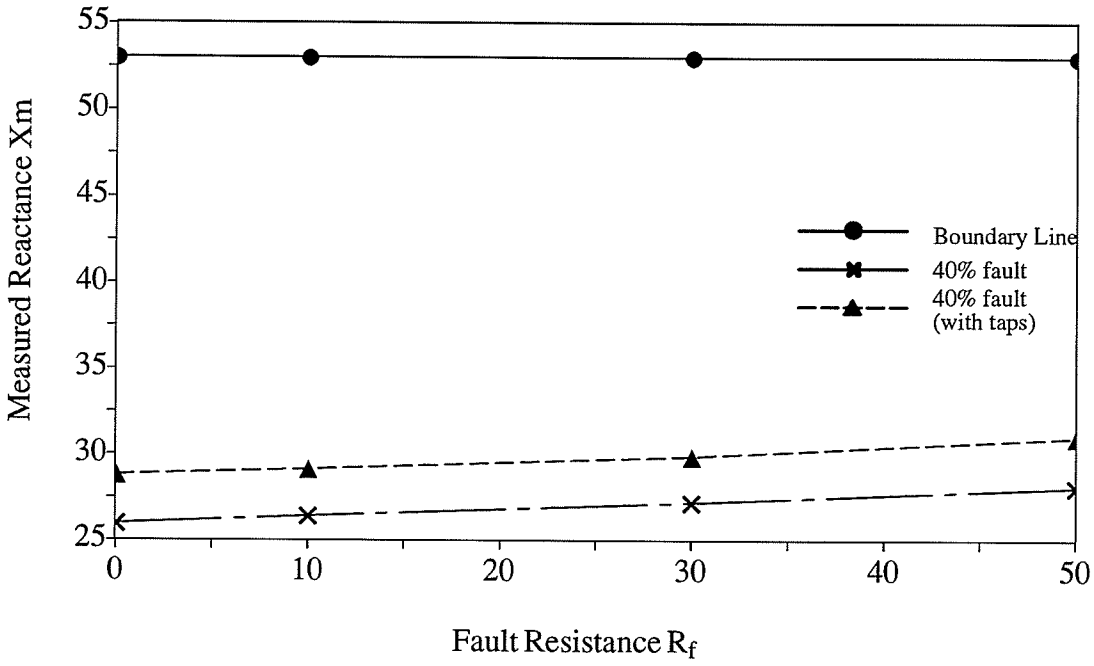

Figure 4.25 40% Single line–to–ground fault At Ponton

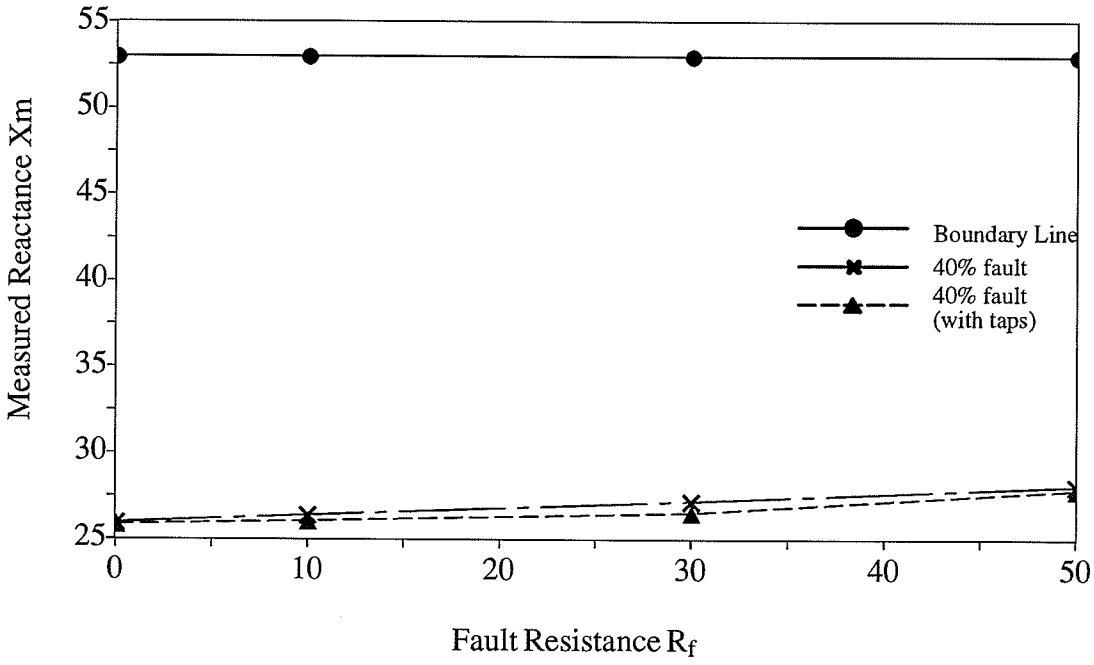

Figure 4.26 40% Single line–to–ground fault At Ponton

To further study the effects of the taps, more tests were done by computer simulation with taps at different locations. It was shown by many tests that a tap with a star–star connection has little effect on the system. The effects are mainly due to the

presence of the taps with a star–delta connection. Moreover, the magnitude of the tap's influence on the system depends on the tap's impedance as well as its position in the system. Figure 4.27 shows the measured reactance under the 78% single line–to–ground fault with different fault resistance conditions when tap 2 is placed at 20% of the line beyond Thompson. Also, Figure 4.28 shows the measured reactance of the 78% fault with different magnitude of tap 2's neutral impedance (25%, 50%, 150% and 200% of the original magnitude). In both cases the original K factor (the one without taps) was used in calculating the reactances. For the case shown in Figure 4.27, the setting of the digital relay was adjusted to accommodate the new system information and the result is shown in Figure 4.29.

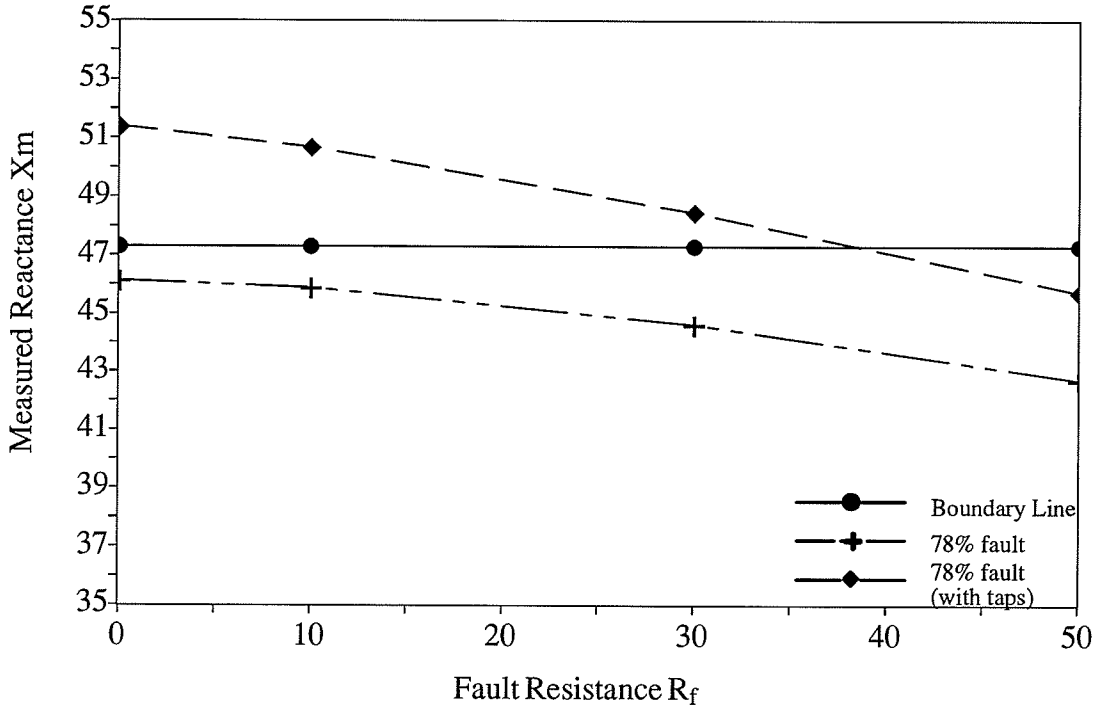

Figure 4.27 78% Single line–to–ground fault (with taps)

change in %	25	50	100	150	200
X_m	61.79	55.73	51.40	49.47	48.75

Table 4–14 measured reactance for 78% ground fault with different tap magnitude

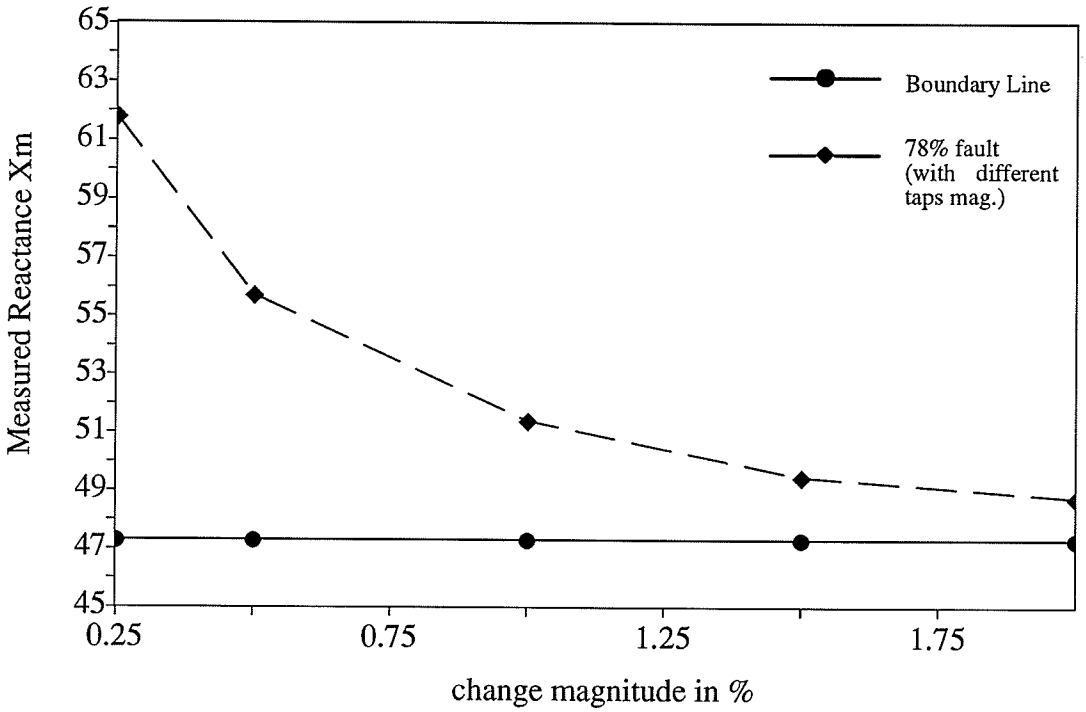

Figure 4.28 78% ground fault with different tap magnitude

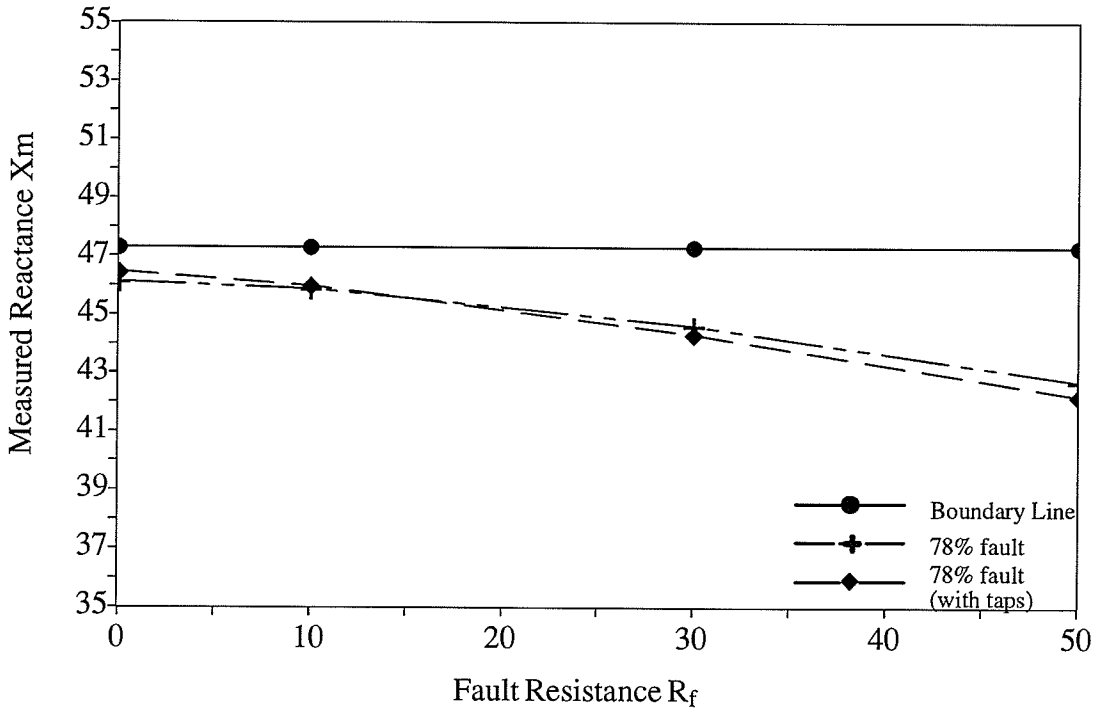

Figure 4.29 78% Single line–to–ground fault (with taps)

One of the attractive features of the digital relaying system is the ability to add or subtract protective functions. This ability is examined in the simulation test. The two proposed adaptive protection features were added into a single digital relay. Single line–to–ground faults were applied at 78% of the line beyond Ponton with Tap 1 and Tap 2 at their original position and the fault resistance was varied from 0 to 50 ohms. Faulted current and voltage were measured at the Ponton end. The result is shown in Figure 4.30. The operating times of the relay are also marked in the figure. It is shown that the two protection schemes can co–exist and improve the performance of the digital relay. As far as the operating time is concerned, there is no obvious time increase when the two schemes are used together. Trip signal can be issued within 2 cycles after the fault was initiated.

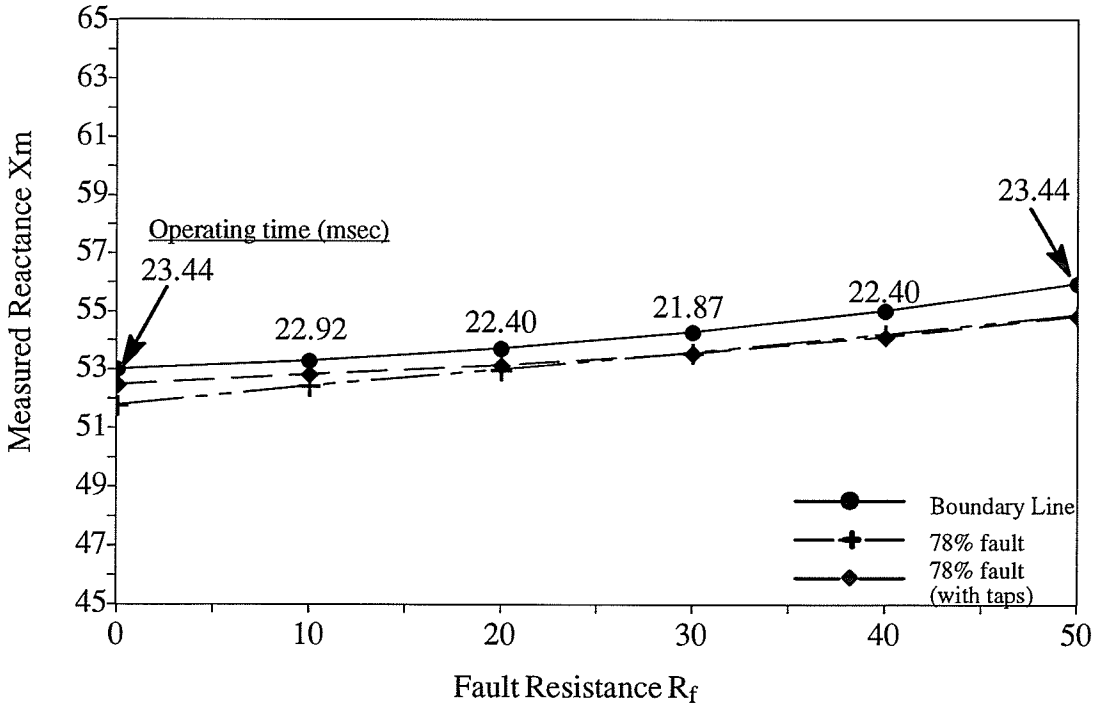

Figure 4.30 78% Single line–to–ground fault (with taps)

4.6 Further considerations

From the simulation results it is believed that the proposed adaptive protection scheme can improve the performance of a distance type relay in a system with taps. However, before the adaptive protection scheme can be applied on the digital relay, an off line system simulation study is required to determine the characteristics of the individual power system. Also, the I_0/I_1 ratio may vary under different load flow conditions. Furthermore, when the power system structure becomes complicated, the distribution of the current in the zero–sequence network also becomes complicated. An adaptive protection method which utilizes the simple I_0/I_1 ratio for decision making may not be suitable under such circumstances. Therefore, more investigation is required to reach a more effective and efficient solution in such cases.

CONCLUSION

It has been shown that the adaptive ground fault protection scheme improves the accuracy in the presence of fault resistance with remote infeed. The digital relay equipped with this adaptive feature is suitable for general application and does not require complex adjustment. The adaptive relay automatically adjusts the remote boundary to provide better protection against single line–to–ground faults which occur near the remote end. The security of the digital relay is not affected by the location of the faults.

A new ground fault protection scheme has also been described which provides a better fault measurement when the transmission system is under the influence of the additional taps. This protection scheme can be achieved through some simple condition checks and the setting of the relay is not significantly more complex. However, when the transmission system structure becomes complicated and the number of tap is increased, this new protection method may not be the perfect solution to the problem. More investigation and work is required to arrive at a better solution.

In conclusion, proposed distance type protection schemes has been evaluated by computer simulation tests. The potential of the adaptive protection schemes for transmission line protection is shown in these tests. Therefore, it is recommended these algorithms be implemented on a digital relaying system for further testing.

APPENDIX I

With reference to Figure 3.2, assuming a single line–to–ground fault of resistance R_f at a proportion m of the total line length, the sequence components of voltage measured at the relay's location are given by :

$$E_1 = I_{1L}(mZ_{1L} + Z_f) + I'_{1L}Z_f \quad (A.1)$$

$$E_2 = I_{2L}(mZ_{2L} + Z_f) + I'_{2L}Z_f \quad (A.2)$$

$$E_0 = I_{0L}(mZ_{0L} + Z_f) + I'_{0L}Z_f \quad (A.3)$$

And we know that

$$E_a = E_1 + E_2 + E_0 \quad (A.4)$$

Therefore, the voltage E_a at the relaying point is the combination of the sequence components of the voltage, which is given by eqn. (A.5).

$$E_a = I_1 mZ_{1L} + I_2 mZ_{2L} + I_0 mZ_{0L} + (I_1 + I_2 + I_0)R_f + (I'_1 + I'_2 + I'_0)R_f \quad (A.5)$$

For $I_a = I_{a1} + I_{a2} + I_{a0}$ and in general, a negative–sequence network has the same impedance as the positive–sequence network and $Z_{2L} = Z_{1L}$. Rearranging terms, eqn. (A.5) can be written in an alternative form :

$$E_a = I_a(mZ_{1L} + R_f) + I'_a R_f + I_0 m(Z_{0L} - Z_{1L}) \quad (A.6)$$

Further examination of eqn. (A.6) reveals that it can be rewritten again as follows :

$$E_a = (I_1 + I_2 + I_0)mZ_{1L} + I_0 m(Z_{0L} - Z_{1L}) + (I_a + I'_a)R_f \quad (A.7)$$

where the variable $(I_a + I'_a)$ is equal to the fault current I_F which flows through the fault resistance branch. Figure A.1 shows the current relations in the fault branch for a single line–to–ground fault.

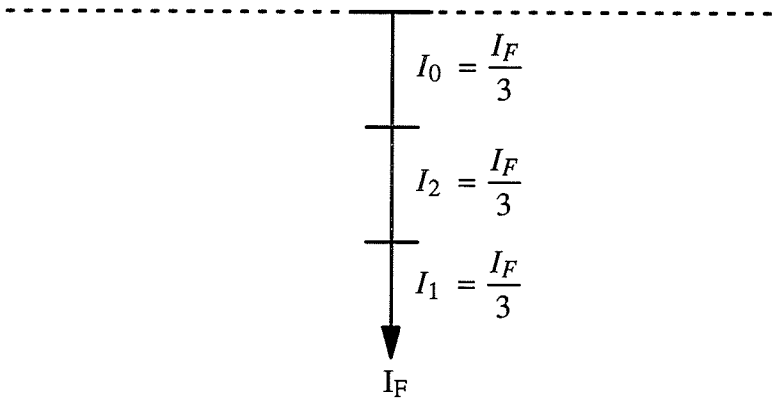

Figure A.1 Current relations for a single line–to–ground fault

$$\frac{1}{3}I_F = I_{1F} = I_{2F} = I_{3F} \tag{A.8}$$

Resolving into sequence components, we have

$$\frac{1}{3}I_F = \frac{1}{3}(I_a + I'_a) = I_1 + I'_1 = I_2 + I'_2 = I_0 + I'_0 \tag{A.9}$$

Since the zero–sequence network is the only sequence network involving an earth grounding, it is logical to let the zero–sequence components be the representation of the fault current and rewrite eqn. (A.7) as :

$$E_a = (I_1 + I_2 + I_0)mZ_{1L} + I_0m(Z_{0L} - Z_{1L}) + 3(I_0 + I'_0)R_f \tag{A.10}$$

Factoring out mZ_{1L} we will have

$$E_a = (I_1 + I_2 + I_0)mZ_{1L} + (\frac{Z_{0L}}{Z_{1L}} - 1)I_0mZ_{1L} + 3(I_0 + I'_0)R_f \tag{A.11}$$

APPENDIX II

With reference to Figure 3.2, assuming a single line–to–ground fault of resistance R_f at a proportion m of the total line length, the measured fault impedance presented to the relay is given by :

$$Z_m = \frac{E_a}{I_a + KI_0} \tag{A.12}$$

With reference to eqn. (A.11), the voltage measured at the relaying point is given as :

$$E_a = (I_1 + I_2 + I_0)mZ_{1L} + (\frac{Z_{0L}}{Z_{1L}} - 1)I_0 mZ_{1L} + 3(I_0 + I_0')R_f \tag{A.13}$$

Factoring out mZ_{1L} and assuming $I_a = I_1 + I_2 + I_0$, $K = \frac{Z_{0L} - Z_{1L}}{Z_{1Z}}$ then

$$E_a = (I_a + KI_0)mZ_{1L} + 3(I_0 + I_0')R_f \tag{A.14}$$

With reference to eqn. (A.12) and eqn. (A.14), now the impedance Z_m is given by :

$$Z_m = mZ_{1L} + \frac{3(I_0 + I_0')}{I_a + KI_0}R_f \tag{A.15}$$

Figure A.2 shows the relationship between zero–sequence currents $I_0 + I_0'$ and I_0 . From the figure, the zero–sequence current $I_0 + I_0'$ is simply related to the measured current I_0 at the relaying point by :

$$I_0 = \frac{Z_{0SB} + (1-m)Z_{0L}}{Z_{SA} + Z_{0SB} + Z_{0L}}(I_0 + I_0') \tag{A.16}$$

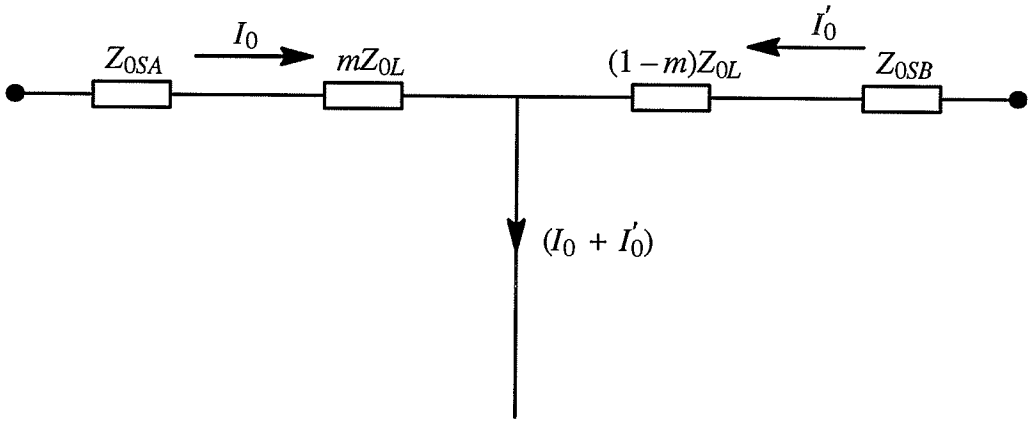

Figure A.2 A circuit model

Substituting the above I_o expression into eqn. (A.15), we have

$$Z_m = mZ_{1L} + \frac{I_0(Z_{0SA} + Z_{0L} + Z_{0SB})3R_f}{(I_a + KI_0)[(1-m)Z_{0L} + Z_{0SB}]} \qquad \text{(A.17)}$$

$$= mZ_{1L} + R_f' \angle\alpha$$

The argument α of the measured impedance Z_{ma} due to R_f is given by :

$$\alpha = \angle I_0 \,/\, (I_a + KI_0) + \angle(Z_{0SA} + Z_{0L} + Z_{0SB}) \,/\, [(1-m)Z_{0L} + Z_{0SB}] \qquad \text{(A.18)}$$

let $\beta = \angle I_0 \,/\, (I_a + KI_0)$ then eqn. (A.18) can be written as :

$$\alpha = \beta + \angle(Z_{0SA} + Z_{0L} + Z_{0SB}) \,/\, [(1-m)Z_{0L} + Z_{0SB}] \qquad \text{(A.19)}$$

Assuming $\theta = \alpha - \beta$, thus θ is given by :

$$\theta = \angle(Z_{0SA} + Z_{0L} + Z_{0SB}) \,/\, [(1-m)Z_{0L} + Z_{0SB}] \qquad \text{(A.20)}$$

APPENDIX III

Fault Type Classification

The Clarke components

With the definition of the Clarke component current from ref. 23 , the following relationships are used to identify the type of the fault.

I_n – neutral current

if $I_n \neq 0$ (ground faults)

For single line–to–ground fault

$I_b - I_c = 0$	phase A to ground fault
$I_a - I_c = 0$	phase B to ground fault
$I_b - I_a = 0$	phase C to ground fault

For double line–to–ground

$2I_a - I_b - I_c + I_n = 0$	phase B and C to ground fault
$2I_b - I_a - I_c + I_n = 0$	phase A and C to ground fault
$2I_c - I_a - I_b + I_n = 0$	phase A and B to ground fault

if $I_n = 0$ (phase faults)

$2I_a - I_b - I_c = 0$	phase B to phase C fault
$2I_b - I_a - I_c = 0$	phase A to phase C fault
$2I_c - I_a - I_b = 0$	phase A to phase B fault

If none of the equalities is satisfied for a phase fault, it is assumed that the fault is a three–phase fault.

It should be point out that while the above equations all involve a zero equality, in the simulation test, a limit band around zero is established.

REFERENCES

[1] A. Wyatt, *Electric Power: Challenges and Choices*, The Book Press, 1986.

[2] Charles A. Gross, *Power System Analysis*, John Wiley & Sons, New York, 1986.

[3] B. Ravindranath and M. Chander, *Power System Protection and Switchgear*, A Halsted Press Book, 1977.

[4] W. D. Stevenson, Jr., *Element of Power System Analysis*, McGraw–Hill, New York, 1982.

[5] A.R. van C. Warrington, "Protective Relays: Their theory and practice (volume one)," Chapman & Hall Ltd., London, 1968.

[6] G. D. Rockefeller, "Fault Protection with a Digital Computer," IEEE Transactions on Power Apparatus and System, vol. 88, pp. 438–464, April 1969.

[7] A. G. Phadke and J. S. Thorp, "Relaying for Power Systems," Research Studies Press Ltd., Somerset, English, 1988.

[8] J. G. Gilbert, E. A. Udren, and M. Sackin, "The Development and Selection of Algorithms for Relaying of Transmission Lines," Power System Control and Protection, Academic Press, 1978.

[9] P. G. McLaren and M. A. Redfern, "Fourier–series Techniques Applied to Distance Protection," PROC. IEE, vol. 122, No. 11, pp. 1301–1305, November 1975.

[10] A. G. Phadke, T. Hlibka and M. Ibrahim, " A Digital Computer System for EHV Substations : Analysis and Field Tests," IEEE Transactions on Power Apparatus and Systems, vol. 95, no. 1, pp. 291–301, January/February 1976.

[11] J. W. Horton, "The Use of Walsh Functions for High–Speed Digital Relaying," IEEE Parer No. A75 582–7, Summer Power Meeting, 1975.

[12] J. G. Gilbert and R. J. Shovlin, "High–Speed Transmission Line Fault Impedance Calculation Using a Dedicated Minicomputer," IEEE Transactions on Power Apparatus and Systems, vol. 94, no. 3, pp. 872–883, May/June 1975.

[13] G. B. Gilcrest, G. D. Rockefeller and E. A. Udren, "High–Speed Distance Relaying Using a Digital Computer; I – System Description" and "II – Test Results," IEEE Transactions on Power Apparatus and Systems, vol. 91, no. 3, pp. 1235–1258, May/June 1972.

[14] A. D. McInnes and I. F. Morrison, "Real–Time Calculation of Resistance and Reactance for Transmission Protection by Digital Computer," E.E. Transactions, Institution of Engineers, Australia, EE7 no. 1, pp. 16–23, 1971

[15] L. W. Couch II, *Digital and Analog Communication Systems*, 2nd, Macmillan, 1987.

[16] Samuel D. Stearns, *Digital Signal Analysis*, Hayden Book Company, Inc., 1975

[17] C. L. Fortescue, "Method of Symmetrical Coordinates Applied to the Solution of Polyphase Networks," Trans. AIEE, vol. 37, pp.1027–1140, 1918.

[18] A. G. Phadke et. al., "Fundamental basis for distance relaying with symmetrical components," IEEE Transactions on Power Apparatus and System, vol. PAS–96, no. 2, pp. 635–646, 1977.

[19] Y. Ohura et. al., "A Digital Distance Relay Using Negative Sequence Current," Paper No. 89 SM 729–5, IEEE PES 1989 Summer Meeting.

[20] W. A. Lewis and L. S. Tippett, "Fundamental Basis for Distance Relaying on a 3–Phase System," Trans. AIEE, vol. 66, pp.694–708, 1947.

[21] Z. Zhang and D. Chen, "An Adaptive Approach in Digital Distance Protection," Paper No. 88 WM 126–5, IEEE PES 1988 Winter Meeting.

[22] A.J Neufeld, E.N Dirks, P.G M^{c}Laren, G.W Swift and R.W. Haywood, "A Microprocessor Platform for a Generic Protection System," 33rd Midwest Symposium on Circuits and Systems, Calgary Convention Centre, Calgary, Alberta, Canada, pp. 377, August 12–15, 1990.

[23] E. Clarke, *Circuit Analysis of AC Power System*, VOl. I, John Wiley & Sons, New York, 1934, Chapter X.

BIBLIOGRAPHY

Fourier Analysis

1. Samuel D. Stearns, *Digital Signal Analysis*, Hayden Book Company, Inc., 1975

2. M. Bellanger, *Digital Processing of Signals: Theory and Practice*, John Wiley & Sons, 1984.

3. W. D. Stanley, G. R. Dougherty and R. Dougherty, *Digital Signal Processing*, 2nd edition, Prentice–Hall, 1984.